CHALMERS
UNIVERSITY OF TECHNOLOGY

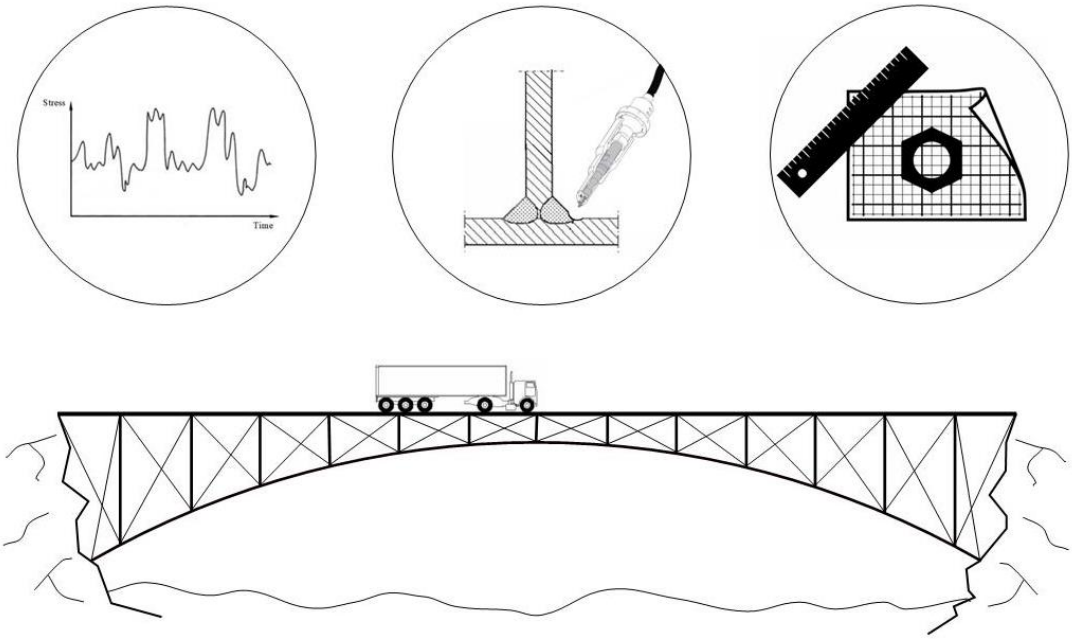

The influence of mean stress in the design with HFMI-treated welds

Investigation of design models to the Eurocode

Master's Thesis in the Masters's Programme Structural Engineering and Building Technology

JOHAN NILSSON

DEPARTMENT OF ARCHITECTURE AND CIVIL ENGINEERING
DIVISION OF STRUCTURAL ENGINEERING

CHALMERS UNIVERSITY OF TECHNOLOGY
Gothenburg, Sweden 2020
www.chalmers.se

MASTER'S THESIS ACEX30

The influence of mean stress in the design of bridges with HFMI-treated welds

Investigation of design models to the Eurocode

Master's Thesis in the Master's Programme Structural Engineering and Building Technology

JOHAN NILSSON

Department of Architecture and Civil Engineering
Division of Structural Engineering
Lightweight Structures
CHALMERS UNIVERSITY OF TECHNOLOGY
Göteborg, Sweden 2020

The influence of mean stress in the design of bridges with HFMI-treated welds
Investigation of design models to the Eurocode

Master's Thesis in the Master's Programme Structural Engineering and Building Technology

JOHAN NILSSON

© JOHAN NILSSON, 2020

Examensarbete ACEX30
Institutionen för arkitektur och samhällsbyggnadsteknik
Chalmers tekniska högskola, 2020

Department of Architecture and Civil Engineering
Division of Division Name
Research Group Name
Chalmers University of Technology
SE-412 96 Göteborg
Sweden
Telephone: + 46 (0)31-772 1000

Chalmers Reproservice / Department of Architecture and Civil Engineering
Göteborg, Sweden, 2020

The influence of mean stress in the design of bridges with HFMI-treated welds

Investigation of design models to the Eurocode

Master's thesis in the Master's Programme Master's Structural Engineering and Building Technology

JOHAN NILSSON

Department of Architecture and Civil Engineering
Division of Structural Engineering
Lightweight Structures
Chalmers University of Technology

ABSTRACT

High-frequency mechanical impact (HFMI) is a post-weld treatment method to increase the fatigue strength of welded components. Most of the research on the performance of HFMI-treated joints has been carried out on structures subjected to constant amplitude loading. However, traffic loads on bridges can generate high and varying mean stresses, which are effects that are not covered by any design recommendations based on these earlier researches. A recent published report suggests a design framework that allows bridge designers to include the effect of mean stress under variable amplitude loading, without information about the stress range spectrum. In this work, traffic simulations are performed to investigate the validity of the suggested design framework, showing that the same results are obtained even for an increased traffic data pool. The same simulations are carried out on Dutch traffic, revealing that the design framework is applicable to traffic situations in other countries than Sweden. Finally, an alternative design framework is developed and presented.

Key words: fatigue; bridge; HFMI, variable amplitude; mean stress; design

Contents

Preface

The work in this Master's Thesis has been carried out between January and June 2020 at the Division of Structural Engineering at Chalmers University of Technology, Gothenburg, Sweden.

I would like to express my gratitude to my supervisor Doctor Poja Shams-Hakimi. His guidelines and supervision have been of great importance to the development of this thesis. I would also like to thank my examiner Professor Mohammad Al-Emrani for his professional input and many ideas.

Gothenburg, June 2020

Johan Nilsson

Notations

AW	as-welded
CA	constant amplitude
FAT	fatigue strength at $2 \cdot 10^6$ cycles
HFMI	high-frequency mechanical impact
IIW	International Institute of Welding
VA	variable amplitude

D	damage factor
f	mean stress correction factor
L	span length
m	slope of *SN* curve
N	number of cycles to failure
R	stress ratio
S	nominal stress
S_{sw}	self-weight stress

ΔS_{eq}	Palmgren-Miner's equivalent stress range
ΔS_{eqR}	equivalent stress range accounting for stress ratio
ΔS_{max}	maximum nominal stress range from traffic
ΔS_{min}	minimum nominal stress range from traffic
ΔS_p	nominal stress range from FLM3
λ_{HFMI}	ratio of ΔS_{eqR} and ΔS_{eq}
Φ	ratio of self-weight stress to maximum stress range from traffic
ξ	ratio of ΔS_{eq} and ΔS_p

1 Introduction

1.1 Background

Steel structures exposed to cyclic loading can be expected to end up in a failure which is caused by initiation and growth of cracks at sensitive locations which over time can lead to structural failure. This is known as fatigue failure and can take place at weldments for load levels below the elastic limit of the material. In addition, fatigue failure can be of brittle nature which can pose a potentially dangerous failure mode in structures exposed to cyclic loading [1].

In the end of 2010, Sweden devolved from designing bridges according to the national design codes, i.e. *Bro 2004* and *BSK 07*, to the new European standards *Eurocode*. The transition resulted in that fatigue, which according to the old standards rarely ended up as the decisive failure mode, to instead became a criterion that could dominate the design of bridge structures. This has caused new steel bridges to require more material than before, leading to loss of competitiveness compared with other materials [2].

Since the fatigue limit state (FLS) more often governs the design, alternatives to conventional bridge designs become relevant. Studies have shown that the combination of high strength steel and post weld treatment can save around 20 % material [3][4]. One of the most efficient post weld treatment techniques is High-Frequency Mechanical Impact (HFMI) treatment. This treatment improves the fatigue strength at the weld toe through high-frequency impacts which introduce compressive residual stresses in fatigue-sensitive locations through plastic deformations. Moreover, the local stress concentration is reduced due to a smoother transition at the weld toe and minor weld defects are eliminated [5].

The International Institute of Welding (IIW) [5] provides design guidelines for the HFMI technique. However, the part of the recommendations concerning the treatment of the mean stress effect is not applicable for bridges, which are subjected to variable amplitude (VA) loading. Shams-Hakimi and Al-Emrani [3][6] therefore proposed an alternative method to account for the mean stress effect which is more suitable for VA loads. Commonly, during the design of bridges, the designer has no information about the detailed traffic data and can therefore not predict the characteristics of the VA load. In order to obtain a usable method for bridge designers, Shams-Hakimi and Al-Emrani also developed a design framework based on measurements of 55,000 Swedish trucks. This design framework will be referred to as the λ_{HFMI}-method in the followings.

1.2 Aim and objectives

The aim of this thesis is to study realistic load effects in bridges and investigate the impact of the mean stresses on the performance of HFMI-treated welds. The following questions defines the objectives of this project.

- To investigate if the 55,000 vehicles, used in the design framework (the λ_{HFMI}-method) by Shams-Hakimi and Al-Emrani, is enough to represent Swedish road traffic in terms of the mean stress effect.

- To investigate the validity and identify potential improvements of the λ_{HFMI}-method.

- To study if the the λ_{HFMI}-method is applicable to traffic in other European countries.

- To study whether the Eurocodes fatigue load models can be used to predict the actual mean stress effect in HFMI-treated bridges.

1.3 Methodology

The first step towards fulfilment of the presented aim and objectives consisted of a literature study. The goal was to provide information about different post weld treatment techniques, in particular the HFMI technique, and also about the effects that VA loading has on HFMI-treated welds. The purpose of the literature study was also to provide information about the design process and fatigue design verification of steel and composite steel/concrete bridges.

With this background, various bridges and bridge models were studied to evaluate the validity of the the λ_{HFMI}-method proposed by Shams-Hakimi and Al-Emrani [3][6]. The programming language Python was used to build functions that can simulate traffic on bridges. The functions retrieved information about the vehicles from a data base and by running these vehicles over bridge influence lines, the response and load effects could be obtained.

The response and load effects were then used to quantify the mean stress effect from the VA spectrum and compare it with the λ_{HFMI}-method and with a modified version of the λ_{HFMI}-method.

Lastly, the load effects caused by Eurocode's fatigue load models 3 and 4 were analysed to investigate the usability of the fatigue load models in predicting the mean stress effect

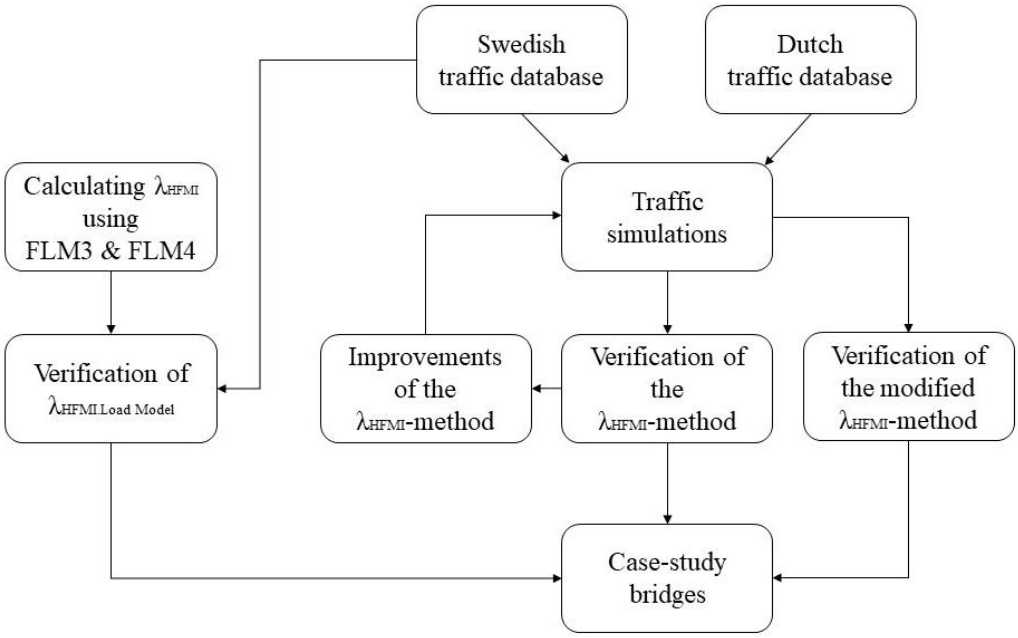

Figure 1.1 Illustration of the methodology.

1.4 Limitations

- The simulations are limited to Swedish and Dutch road traffic.
- The thesis focuses on fatigue improvement of new bridges with HFMI treatment and does not include aspects of repair or retrofitting of existing structures.
- All the bridges investigated in the thesis are girder bridges.

2 Fatigue design of steel and composite bridges

2.1 Fatigue load models in Eurocode

Traffic on bridges generates a stress range spectrum, which may result in fatigue failure. The spectrum is dependent of the geometry of the vehicles, the axle loads, the distance between the vehicles, the composition of the traffic and its dynamic effects. In order to represent the complex load effects generated by traffic load, Eurocode defines five fatigue load models.

2.1.1 Fatigue load model 1

Fatigue load model 1 (FLM1) is composed in the same manner as the characteristic load model 1 (LM1), which is used for ultimate limit state verification, with the difference that the concentrated axle loads and the distributed load are reduced by a factor of 0.7 and 0.3 respectively, see Figure 2.1 and Table 2.1. The model generates a constant amplitude stress range were the minimum and the maximum stresses should be determined by different possible placements of the load on the bridge. The model is intended to check whether the fatigue life of the bridge may be considered infinite [7].

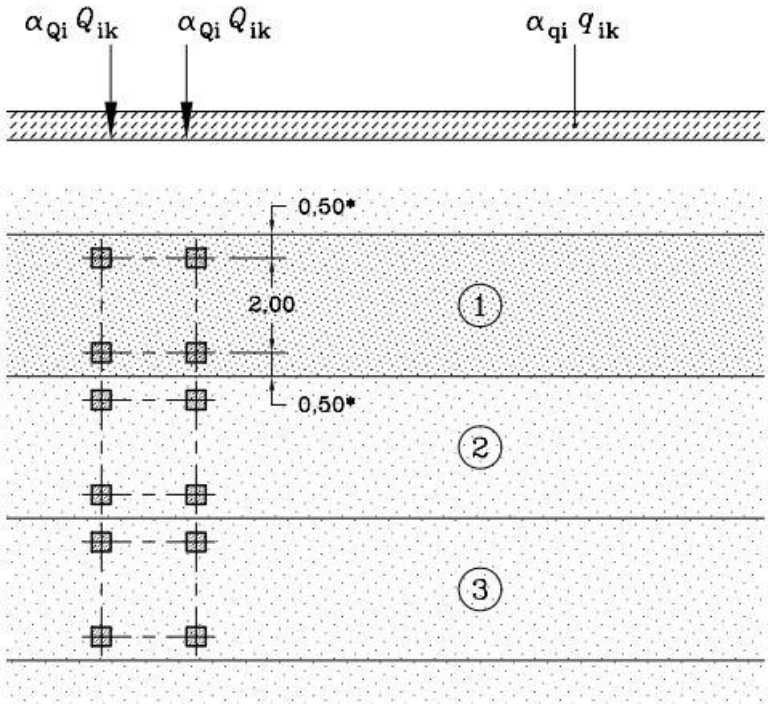

Figure 2.1 Details for FLM1, adapted from EN 1991-2:2003 [7].

Table 2.1 Concentrated axle loads and distributed loads for FLM1, according to EN 1991-2:2003 [7].

Lane Number	Q_{ik} [kN]	q_{ik} [kN/m^2]
1	210	2.7
2	140	0.75
3	70	0.75

2.1.2 Fatigue load model 2

Fatigue load model 2 (FLM2) is defined as a set of idealized lorries, called frequent lorries. It consists of five different vehicles with different axle loads and axle spacings, see Table 2.2. Similar to FLM1, FLM2 is intended to be used if the fatigue life time is designed to be infinite [7].

Table 2.2 Frequent lorries (FLM2), according to Table 4.6 in EN 1991-2:2003 [7].

LORRY	Axle Spacing [m]	Frequent Axle Loads [kN]	Axle Type
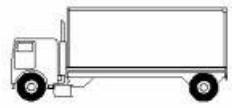	4.5	90 190	A B
	4.20 1.30	80 140 140	A B B
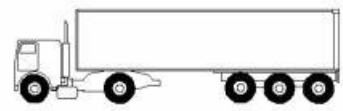	3.20 5.20 1.30 1.30	90 180 120 120 120	A B C C C
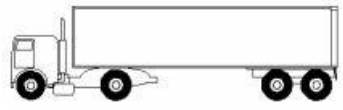	3.40 6.00 1.80	90 190 140 140	A B B B
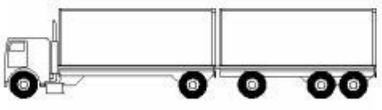	4.80 3.60 4.40 1.30	90 180 120 110 110	A B C C C

2.1.3 Fatigue load model 3

Fatigue load model 3 (FLM3) consists of one vehicle with four axles, see Figure 2.2. The force of each axle is 120 kN and each tire has a contact surface represented by a square with a length of 0.40 m [7]. FLM3 is intendent to be used with the simplified λ-method, see Section 2.2, where the calculated stress range should be less than or equal to the fatigue strength of the investigated weld detail [8]

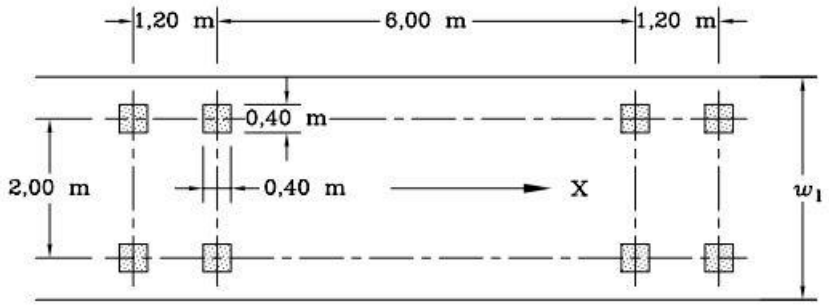

Figure 2.2 Geometry of fatigue load model 3, adapted from [7].

2.1.4 Fatigue load model 4

Fatigue load model 4 (FLM4) consists of a set of five standardized vehicles, which are consistent with the most common heavy vehicles on European roadways [8]. In addition, FLM4 includes three different traffic types where the proportion of the lorries vary, representing local traffic, medium distance traffic and long-distance traffic, see Table 2.3. Similar to FLM3, FLM4 is intended to be used for verification for finite fatigue life [7].

Table 2.3 Geometry and distribution of the lorries in FLM4, according to Table 4.7 in EN 1991-2:2003 [7].

VEHICLE TYPE			**TRAFFIC TYPE**			
			Long distance	**Medium distance**	**Local traffic**	
LORRY	**Axle Spacing** [m]	**Equivalent Axle Loads** [kN]	**Lorry percentage**			**Axle Type**
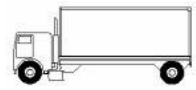	4.5	90 190	20.0	40.0	80.0	A B
	4.20 1.30	80 140 140	5.0	10.0	5.0	A B B
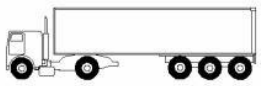	3.20 5.20 1.30 1.30	90 180 120 120 120	50.0	30.0	5.0	A B C C C
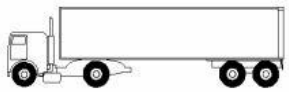	3.40 6.00 1.80	90 190 140 140	15.0	15.0	5.0	A B B B
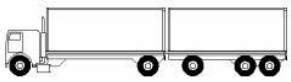	4.80 3.60 4.40 1.30	90 180 120 110 110	10.0	5.0	5.0	A B C C C

2.1.5 Fatigue load model 5

Fatigue load model 5 (FLM5) is based on measured traffic data. The data is supplemented with statistical extrapolations to accommodate future traffic increases [7]. FLM5 is intended to be used to verify the fatigue strength of complex bridges or bridges with unusual traffic [8].

2.2 Fatigue verification methods

Eurocode defines two methods for fatigue verification in bridges.

2.2.1 The λ-coefficient method

The equivalent damage method, also known as the λ-coefficient method, is a simplified method. The idea is that the fatigue damage caused by the actual stress range spectrum from traffic can be described by one equivalent stress range which is obtained with a damage equivalent factor [8]. The largest stress range generated by fatigue load model 3, ΔS_p, is multiplied by a factor λ in order to represent the equivalent stress range from real traffic $2 \cdot 10^6$ stress cycles, see Equation (2.1).

$$\Delta S_{E,2} = \lambda \cdot \phi_2 \cdot \Delta S_p \tag{2.1}$$

Where;
λ is the fatigue damage equivalent factor related to $2 \cdot 10^6$ cycles;
Φ_2 is the damage equivalent dynamic factor.

The fatigue damage equivalent factor, for road bridges, is obtained by Equation (2.2). The λ-coefficients are presented in EN 1993-2 Section 9.5.2.

$$\lambda = \lambda_1 \cdot \lambda_2 \cdot \lambda_3 \cdot \lambda_4 \leq \lambda_{max} \tag{2.2}$$

Where;
λ_1 is the span factor, considering the length of the critical influence line;
λ_2 is the factor considering the traffic volume;
λ_3 is the factor considering the design life of the bridge;
λ_4 is the factor considering traffic in additional lanes;
λ_{max} is maximum λ-value considering the fatigue limit.

The equivalent stress range should be verified against the fatigue strength of the studied detail category, according to Equation (2.3).

$$\gamma_{Ff} \cdot \Delta S_{E2} \leq \frac{\Delta S_c}{\gamma_{Mf}} \tag{2.3}$$

Where;
γ_{Ff} is the partial safety factor for fatigue loading;
γ_{Mf} is the partial factor for fatigue resistance.

2.2.2 Palmgren-Miner's damage accumulation method

A stress range spectrum generated by traffic loads can be very complex, with varying magnitude and frequency. A stress range spectrum such as in Figure 2.3 should be transformed into one or more equivalent constant amplitudes that generate an equivalent fatigue damage as the real loading situation. This can be done by first transforming the variable amplitude load history into individual load cycles using cyclic count methods such as the rainflow- or the reservoir counting method [1].

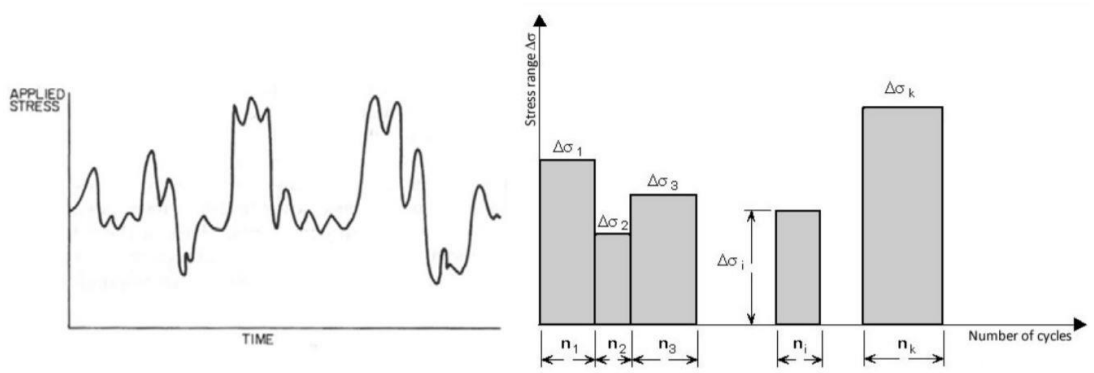

Figure 2.3 To the left: Stress range spectrum with variable amplitude. To the right: The resulting histogram using a cyclic counting method, adapted from [1].

Performing the fatigue design can be done by applying the Palmgren-Miner damage accumulation rule to the obtained stress ranges from the cycle counting. The method is based on the assumption that the fatigue damage is cumulative and irreversible. In other words, the fatigue life, represented by an S-N curve, for a certain detail is consumed after N cycles of a certain stress range [1]. If the number of stress cycles $n < N$, the accumulated damage can be calculated as:

$$D = \frac{n}{N} \tag{2.4}$$

With a spectrum as shown in Figure 2.3, with a number i loading blocks with a certain stress range, $\Delta\sigma_i$, and corresponding number of cycles, n_i, the total accumulated fatigue damage is obtained by the sum of the fatigue damage caused by each individual loading block, see Equation (2.5).

$$D = \sum_i D_i = \sum_i \frac{n_i}{N_i} \tag{2.5}$$

Where N_i is the number of cycles that would cause damage for a certain stress range, $\Delta\sigma_i$, see Equation (2.6).

$$N_i = 5{\cdot}10^6 \left(\frac{\frac{\Delta\sigma_D}{\gamma_{Mf}}}{\gamma_{Ff} \cdot \Delta\sigma_i} \right)^m \tag{2.6}$$

For a design curve with a constant slope, m, the same damage, D, is caused by the equivalent stress range, $\Delta\sigma_E$, after the same total number of cycles, i.e.

$$D_E = \frac{\sum_{i=1}^{n} n_i}{N} = \frac{\Delta\sigma_E^m}{5{\cdot}10^6 \cdot \Delta\sigma_D^m} \cdot \sum_{i=1}^{n} n_i \tag{2.7}$$

Which also can be expressed in terms of equivalent stress:

$$\Delta\sigma_E = \sqrt[m]{\frac{\sum_{i=1}^{n} n_i \cdot \Delta\sigma_i^m}{\sum_{i=1}^{n} n_i}} \tag{2.8}$$

For a histogram composed of several stress blocks with different stress ranges, the equivalent stress range can be expressed as:

$$\Delta\sigma_E = \sqrt[mi]{\frac{\sum n_i \Delta\sigma_i^{m_i} + \sum n_j \Delta\sigma_j^{m_i} (\frac{\Delta\sigma_j}{\Delta\sigma_D})^{m_j - m_i}}{\sum n_i + \sum n_j}} \tag{2.9}$$

Where;

i is the index of stress ranges larger than $\Delta\sigma_D$,
j is the index of stress ranges smaller than $\Delta\sigma_D$,
m_i is the slope of the tri-linear S-N curve above the knee point,
m_j is the slope of the tri-linear S-N curve below the knee point.

3 Post Weld Treatment (PWT) methods

In order to enhance the fatigue life of a welded structure it is important to apply good design practice. However, in situations where critical detailing cannot be avoided post weld improvements techniques can be used [5].

3.1 Classification of PWT methods

Post weld treatment (PWT) techniques generally either modify the weld geometry or alter the residual stress state to become more beneficial in terms of fatigue. The aim with the modification of the weld geometry is to reduce local stress peaks by creating a smoother transition between the weld and the base plate, and improve the surface quality by eliminating weld defects such as undercuts [5].

3.1.1 Weld geometry improvement methods

Weld geometry improvement methods can further be divided into two sub-categories as shown in Figure 3.1.

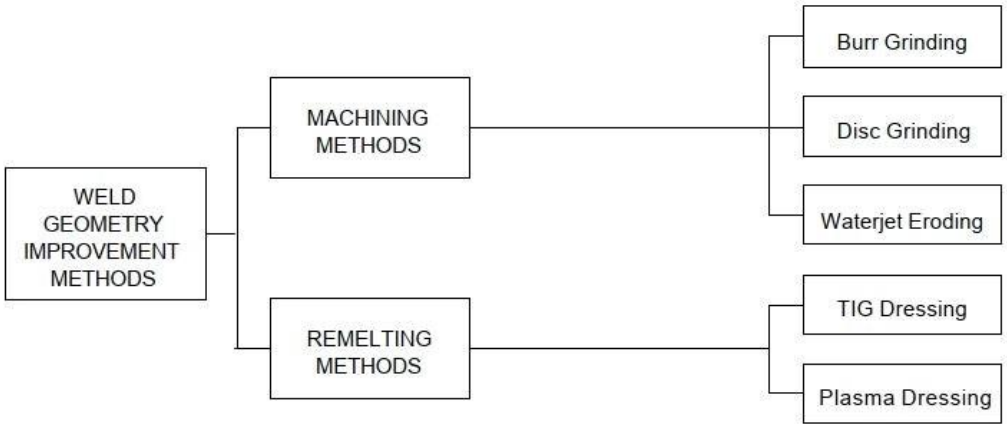

Figure 3.1 Classification of weld geometry improvement methods. Adopted from [9].

3.1.1.1 Grinding methods

The aim of grinding is to reduce stress concentrations by creating a smoother transition between the weld toe and the base metal and by removing weld defects and undercuts at the weld toe. The largest improvements of the fatigue strength is obtained for high strength steel [9]. Grinding improves the fatigue life with a factor of 1.3 compared with the as-welded state [10].

3.1.1.2 Re-melting methods

These techniques result in a re-melted area at the weld toe region. This creates a smoother transition between the weld toe and the base metal without undercuts and slag inclusions [9]. Tungsten Inert Gas (TIG) dressing can improve the fatigue strength by a factor of 1.3 [10]. Re-melting methods are suitable for automation. However, it is

difficult to ensure that the result of the re-melting has been accomplished appropriately [9].

3.1.2 Residual stress methods

Residual stress methods can further be divided into three sub-categories, peening-, overloading- and thermal methods, as shown in Figure 3.2.

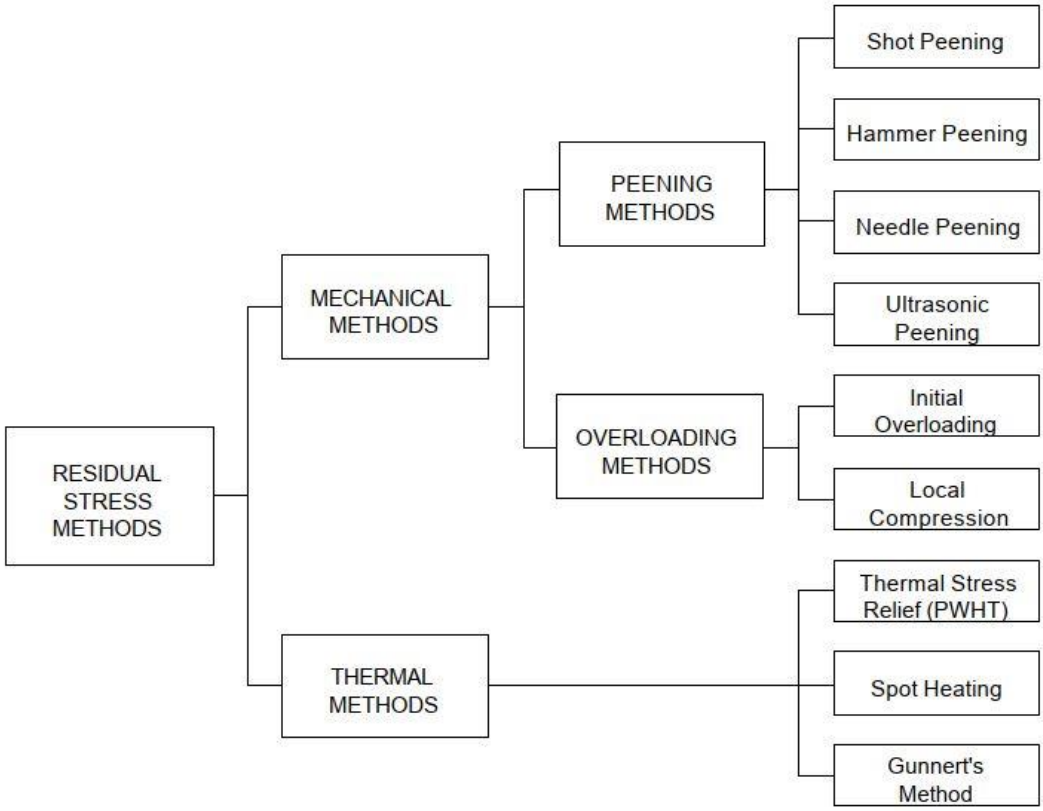

Figure 3.2 Classification of residual stress methods. Adapted from [9].

3.1.2.1 Peening methods

Peening is a cold working technique which plastically deforms the welded region through impacts. This replaces the tensile residual stresses from the welding process with favorable compressive residual stresses. The magnitude of the compressive stresses is of the order of the yield stress of the material. The fatigue strength improvement becomes greater the higher the strength steel. In addition to the induced compressive residual stresses, the transition and weld undercuts at the weld toe are smoothened out [9]. Both hammer- and needle peening improves the fatigue strength by a factor of 1.3 for $f_y < 355$ MPa and a factor of 1.5 for $f_y \geq 355$ MPa [10].

3.1.2.2 Overloading methods

Overloading methods is classified as mechanical methods, just as peening. Prior to fatigue loading, static overloading can introduce compressive residual stresses at the weld toe by local yielding in the range of 50 % to 90 % of the yield stress [9].

3.1.2.3 Thermal methods

The primary aim of thermal methods is to remove tensile residual stresses by introducing heat to the welded region [9]. When using thermal stress relief, the material is heated to a temperature between 550 ℃ to 650 ℃. After a specified amount of time, the material is cooled down in a controlled manner in order to not create new tensile residual stresses [11].

3.2 High Frequency Mechanical Impact (HFMI)

In 2010, Commission XIII of the IIW [5] introduced the term high frequency mechanical impact (HFMI) as a generic term to describe several related peening technologies developed by different equipment manufacturers. The devices operate similar to the older hammer- and needle peening tools but in general, the impact frequencies are higher. The IIW defines the HFMI technologies to have impact frequencies greater than 90 Hz.

This thesis focuses on the HFMI treatment. All results in Chapter 4, 5, 6 & 7 are related to this technique.

3.2.1 Description of the process

Similar to hammer and needle peening, the HFMI equipment accelerates single or multiple indenters against the weld toe region. The indenters cause plastic deformation in the material which results in a change in geometry as well as compressive residual stresses in the impacted area. The higher impact frequency of the HFMI treatment leads to a greater treatment quality compared with the older methods since smaller spacing between the indentations are generated which gives a smoother surface [12].

3.2.2 Influence of loading

Since high tensile residual stresses already exists at the weld toe of as-welded (AW) joints, the fatigue strength is considered to be independent of load conditions, such as high mean stress or maximum loads. The tensile residual stresses, which are of the order of the yield stress, makes the local mean stress insensitive to changes in the subjected load. The maximum loads can even result in a beneficial effect of the AW joint. Due to the high stress concentrations at the weld toe, the overload events in VA loading can cause local yielding and relax the existing residual stresses [3].

On the other hand, one of the mechanisms that improves the fatigue life of HFMI-treated joints is the induced compressive residual stresses. When the tensile mean stress increase, the compressive residual stresses reduces which making the following load cycles more damaging. Overloads in VA-loading, e.g. due to high dead load or individual large stresses, may result in that the structure yield locally and release the compressive residual stresses permanently [13].

3.2.3 Design framework

In order not to affect the induced residual stresses, the international institute of welding (IIW) [5] provides a maximum permissible stress range as a function of the stress ratio, which can be seen in Figure 3.3. The stress ratio is an alternative representation of the mean stress and is defined as the ratio of minimum to maximum stress of a cycle. If the largest stress range exceeds the limit value for a given yield stress, the benefit of HFMI cannot be claimed without fatigue testing [5].

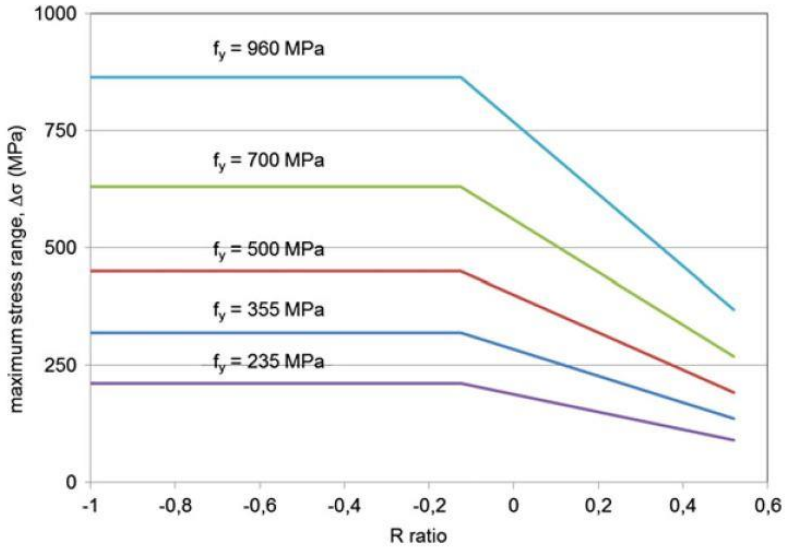

Figure 3.3 Limitation on maximum stress range, adapted from [5]

IIW also provides an approach to account for the effect of high mean stress. The stress ratio impact is formulated as penalties on the fatigue strength (FAT) class, for different intervals of stress ratio. These are given in Table 3.1.

Table 3.1 Reduction of FAT class for HFMI treated welded joints for increased stress ratio, according to the IIW [5].

Stress ratio, R	Minimum FAT class reduction
$R \leq 0.15$	No reduction
$0.15 < R \leq 0.28$	1 FAT class
$0.28 < R \leq 0.40$	2 FAT classes
$0.40 < R \leq 0.52$	3 FAT classes

This method is suitable for CA applications where the mean stress remains constant during the loading, but due to its stepwise function and lack of data, for $R > 0.52$, it is less suitable for VA loading if the mean stresses vary. More specifically, no single S-N curve is valid when the stress ratios vary within the same loading.

Shams-Hakimi and Al-Emrani [3][6] suggested a modification of the IIW stress ratio correction in order to make it suitable for VA applications in bridges, which were found to include varying stress ratios for different cycles. Instead of reducing the fatigue strength for every individual cycle, the strength was kept constant as the CA R=0.1 strength. The stress ranges were then magnified with a correction factor of approximately 1.125 for every FAT class that would be reduced according to the IIW method, see Figure 3.4. In addition, they also extrapolated the method to R=1.0 and a polynomial fit was performed to generate a continuous expression, see Equation 3.1. The continuous expression allows the Palmgren-Miner's equivalent stress range, Equation (3.2), to be modified to include the stress ratio effect, see Equation (3.3).

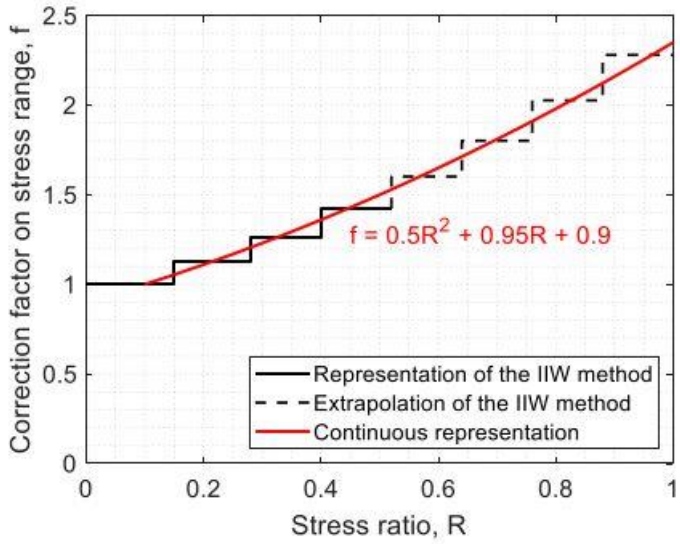

Figure 3.4 The IIW stepwise method together with Shams-Hakimi and Al-Emrani's [3][6] suggested mean stress correction, adapted from [6].

$$f_i = 0.5R_i^2 + 0.95R_i + 0.9 \tag{3.1}$$

$$\Delta S_{eq} = \sqrt[m]{\frac{\sum(n_i \cdot \Delta S_i{}^m)}{\sum n_i}} \tag{3.2}$$

$$\Delta S_{eqR} = \sqrt[m]{\frac{\sum(n_i \cdot (\Delta S_i \cdot f_i)^m)}{\sum n_i}} \tag{3.3}$$

3.2.3.1 Design framework for bridges

At present, there are no design methods for HFMI-treated joints included in the Eurocodes. The most common fatigue verification of AW joints, in the Eurocodes is the lambda method. As mentioned in the previous chapter, in Section 2.2.1, the lambda method is carried out by calculating the stress range, ΔS_p, generated by the fatigue load model 3 (FLM3) [14]. To obtain the equivalent stress range from the real traffic, ΔS_p is multiplied with a set of λ factors that include the span length factor, the volume of the traffic, the intended service life of the bridge and a factor for traffic in more than one lane.

To cover HFMI-treated joints, Shams-Hakimi and Al-Emrani [3][6] suggests an extension of the method, by adding a new factor λ_{HFMI}. The factor needs to include the stress ratio variation of the real traffic and the effect of self-weight as well as the relationship of the fatigue strength to the mean stress or stress ratio. The suggested λ_{HFMI} factor is the ratio of the modified equivalent stress range, ΔS_{eqR}, and the equivalent stress range ΔS_{eq}, see Equation (3.4).

$$\lambda_{HFMI} = \frac{\Delta S_{eqR}}{\Delta S_{eq}} \tag{3.4}$$

The VA load is not known by the designer and thereby, neither is the modified equivalent stress range, ΔS_{eqR}. To be able to predict λ_{HFMI}, Shams-Hakimi and Al-Emrani [3][6] used 55,000 measured Swedish vehicles to calculate the factor for different spans, support conditions and self-weights. The results were simplified into two different equations, one for span sections, Equation (3.5), and one for support sections, Equation (3.6). λ_{HFMI} varies with a factor ϕ, which is the ratio of the stress caused by the self-weight, S_{SW}, and the largest stress range caused by the real traffic, ΔS_{max}, see Equation (3.7). ΔS_{max} was found to be approximately equal to $2\Delta S_p$, see Figure 3.5. The benefit of relating this quantity to ΔS_p is that this parameter is known to the designer and therefore does not require additional analyses.

$$\lambda_{HFMI} = \frac{2.38\phi + 0.64}{\phi + 0.66} \tag{3.5}$$

$$\lambda_{HFMI} = \frac{2.38\phi + 0.06}{\phi + 0.40} \tag{3.6}$$

$$\Phi = \frac{S_{SW}}{\Delta S_{max}} \tag{3.7}$$

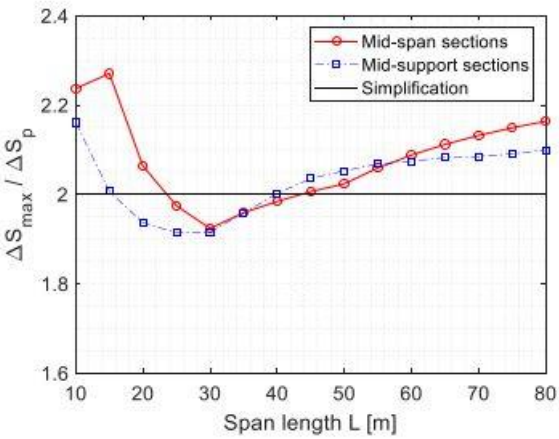

Figure 3.5 Ratio of maximum stress range and the stress range from FLM3, adapted from [6].

4 Validity of the traffic data

The λ_{HFMI}-method, proposed by Shams-Hakimi and Al-Emrani [3][6], is limited to Swedish road traffic. 55,000 Swedish vehicles were used as a representation for the real traffic.

In this chapter, it is investigated whether the traffic data pool, used by Shams-Hakimi and Al-Emrani [3][6], is large enough to represent Swedish road traffic. In addition, a comparison with traffic data from the Netherlands was made in order to consider if the Swedish traffic data is representative for other European countries.

4.1 Increased traffic data pool

To ensure that the traffic data of 55,000 vehicles is enough to represent Swedish road traffic, the same methodology to derive λ_{HFMI} was performed with a larger traffic pool.

4.1.1 The Swedish traffic data pool

The calculations are based on traffic measurements performed by The Swedish Road Administration during the years 2005 to 2009. The sorted and processed traffic data has been obtained from Prof. John Leander and previous work related to this data was published by Leander [15]. The measurements are performed by the technique Bridge Weight in Motion (BWIM), where a bridge together with strain gauges are used as a scale to characterize the vehicles when they pass by. The traffic data contains 872,090 vehicles, measured at different locations distributed over the whole country.

4.1.2 Result

The vehicles were driven over a 10 meter simply supported bridge and a continuous two span bridge with equal span lengths of 10 meter. Shams-Hakimi and Al-Emrani [3][6] made simulations on various span lengths and conclude that the most conservative result was obtained for the shortest spans. This is since a short span bridge can generate additional secondary cycles while a longer bridge mainly generates one cycle per vehicle. The additional cycles tend to have a higher minimum stress compared with the main cycles and therefore contribute to a higher mean stress effect. As mentioned in Chapter 3, the expression of λ_{HFMI} was simplified to one equation for span sections and one equation for mid-support sections. The locations that were found to represent the two different sections were in $0.50L$ of a simply supported bridge and $0.85L$ of a symmetric double-span bridge. An S-N slope of $m = 5$ was used to calculate both the Palmgren-Miner's equivalent stress range, ΔS_{eq}, and the modified equivalent stress range, ΔS_{eqR}, according to Equation (3.3) [3][6].

Figure 4.1 shows a comparison of the generated Φ-λ_{HFMI} curves for the larger Swedish data pool with the expressions for λ_{HFMI} according to equation (3.5) and (3.6). The equations purposed by Shams-Hakimi and Al-Emrani [3][6] produce equal or conservative λ_{HFMI}-values for all Φ except for $\Phi \approx 2$ in the support section, where the real traffic of the larger Swedish data pool generated a maximum difference of 1.03 %.

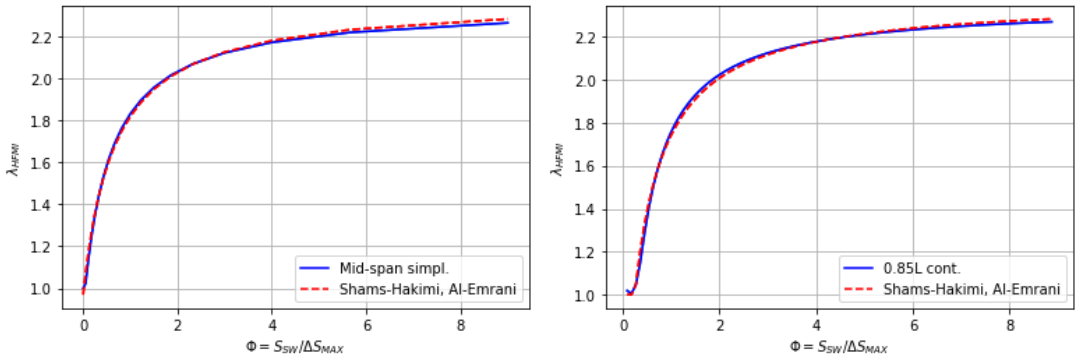

Figure 4.1 *Comparison of Φ-λ_{HFMI} curves calculated with 872,090 Swedish vehicles and the equations (3.5 and 3.6) suggested by Shams-Hakimi and Al-Emrani [3][6]. To the left: Mid-span sections. To the right: Support sections.*

4.2 Comparison with Dutch traffic data

To study if the Swedish traffic is capable of representing λ_{HFMI} for other European countries as well, traffic data from the Netherlands was also tested.

4.2.1 The Dutch traffic data pool

The Dutch traffic data has been obtained from Prof. Johan Maljaars and will be published in [16]. The data consists of two different traffic pools which were measured during April 2008 and April 2018, respectively, at highway A16 in the Netherlands. The measurements were performed by Weight in Motion (WIM), which is a pavement-based technique using sensors embedded in the pavement to measure the forces caused by the vehicles. All vehicles that exceeded the maximum permitted gross weight have been removed in the measurements from 2008 [16]. That is not done for the measurements from 2018. The databases from 2008 and 2018 contains 238,133 and 239,403 vehicles respectively.

4.2.2 Result

A comparison of the stress range spectrum generated by the Dutch traffic is made with the spectrum of the larger traffic pool from Sweden for the mid-span section of a 30 m simply supported bridge, see Figure 4.2. Some similarities of the trends in the distributions is observed, however, the Swedish spectrum contained a greater proportion of large stress ranges compared with the Dutch spectrum from 2008 and 2018.

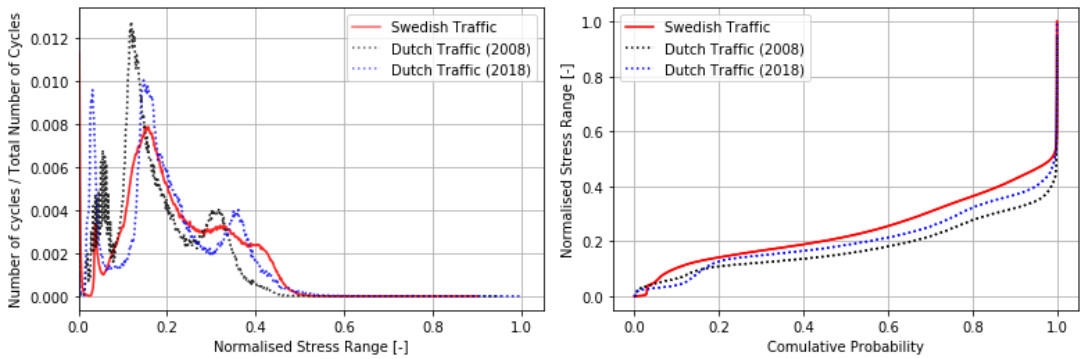

Figure 4.2 *Comparison of Swedish and Dutch (2008 & 2018) normalised stress range spectrum as a histogram (to the left) and a cumulative frequency distribution (to the right).*

Apparently, the differences in the stress range spectra did not affect the mean stress effect too much. Equation (3.5) and (3.6) were compared with generated Φ-λ_{HFMI} curves for Dutch traffic (2008) and the equations produced higher λ_{HFMI} for all ϕ with a maximum discrepancy of 2.6 %, see Figure 4.3. The different traffic of the two countries resulted in a maximum discrepancy of 2.6%, where the equation proposed by Shams-Hakimi and Al-Emrani was conservative for all ϕ, see Figure 4.3.

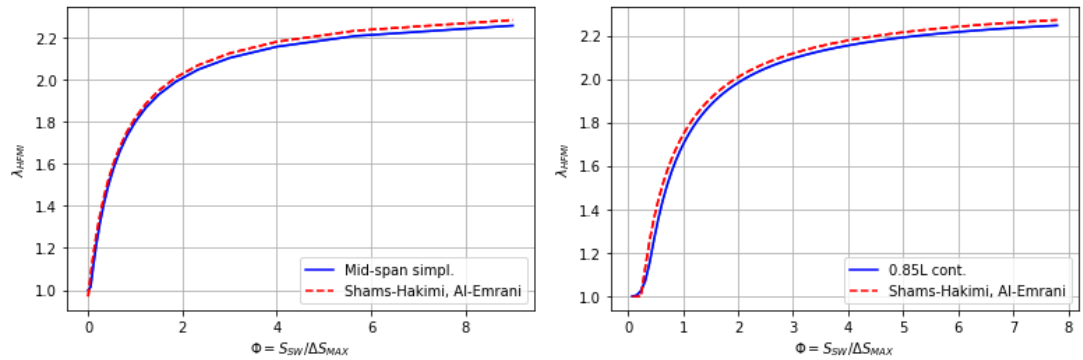

Figure 4.3 *Comparison of Φ-λ_{HFMI} curves calculated with Dutch vehicles (2008) and the equations suggested by Shams-Hakimi and Al-Emrani [3][6]. To the left: Mid-span section. To the right: Support sections.*

4.2.3 Sensitivity of the method to maximum stress range

The Dutch database, from 2018, was unsorted and contained vehicles that exceeded the maximum allowed gross weight and thereby needed special permission to travel on the Dutch roads. The stress history of the 2018 traffic data therefore contained an abnormal overload that was 20 % larger compared with the maximum stress for the traffic from 2008, see Figure 4.4.

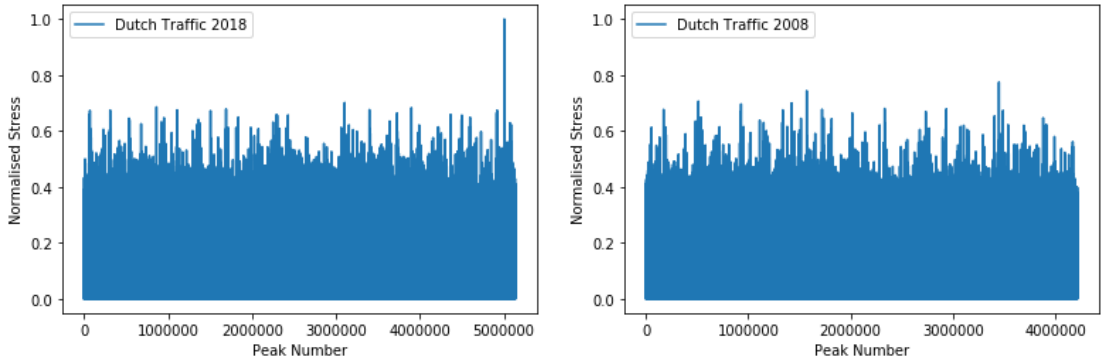

Figure 4.4 *Normalised stress history generated by the database from 2018 (to the left) and by the database from 2008 (to the right).*

Figure 4.5 reveals that the Dutch traffic from 2018 produces higher Φ-λ_{HFMI} curves compared with equations (3.5) and (3.6) due to the abnormally large ΔS_{max}. This reveals a sensitivity of this method of representing λ_{HFMI} and justifies a redefinition of Φ in order to compare the different databases in a representative manner. Of course, a better way of comparing the 2018 database to the proposed equations by Shams-Hakimi and Al-Emrani [3][6] would be to exclude the extreme vehicles since this would make a negligible difference in the actual mean stress effect. The simulation of the Dutch traffic data from 2018 generated a maximum difference of λ_{HFMI} that was 9 % higher than predicted with Equation (3.5) and (3.6).

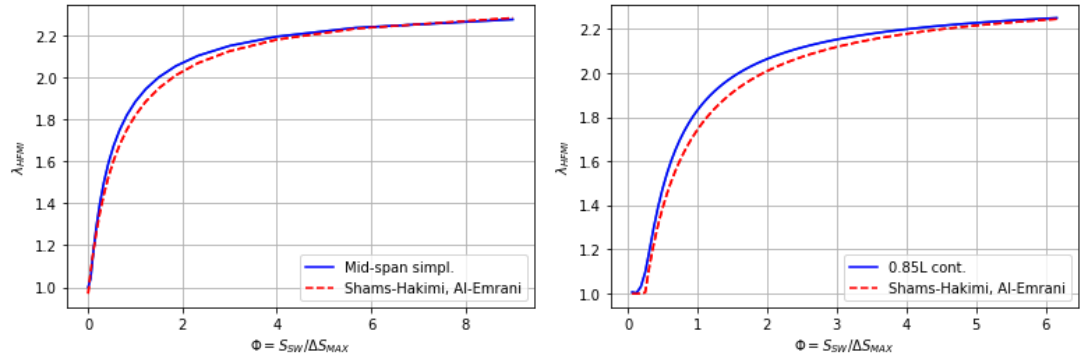

Figure 4.5 *Comparison of Φ-λ_{HFMI} curves calculated with Dutch vehicles, measured during April 2018, and the equation suggested by Shams-Hakimi and Al-Emrani [3][6]. To the left: Mid-span section. To the right: Support sections.*

5 Improvements of the Method

The results obtained in Chapter 4 have shown that the 55,000 vehicles that Shams-Hakimi and Al-Emrani [3][6] used was enough to represent Swedish road traffic in a satisfactory manner. It was also shown that the method was applicable to Dutch traffic data from 2008 as well. On the other hand, the results showed that the method was sensitive to abnormal overloads, therefore, a good comparison to the 2018 Dutch traffic data could not be made.

In this chapter the same methodology will be performed, with the aim of altering the method to become less sensitive to changes of the maximum stress range.

5.1 New definition of Φ

λ_{HFMI} depends on the factor ϕ which is the ratio of the stress caused by the self-weight and the maximum stress range produced by the traffic, see Equation (3.7). To make the method less sensitive to the stress range of a single vehicle, Φ needs to be redefined.

Palmgren-Miner's equivalent stress range, ΔS_{eq}, is a factor that represents all the vehicles in the stress range spectrum and is therefore insensitive to the stress range generated by a single vehicle. By redefining Φ as the ratio of the stress caused by the self-weight and Palmgren-Miner's equivalent stress range, see Equation (5.1), the aforementioned sensitivity of λ_{HFMI} to ΔS_{max} is eliminated.

$$\Phi = \frac{S_{SW}}{\Delta S_{eq}} \tag{5.1}$$

In the followings, Φ-λ_{HFMI} curves are produced with the new definition of Φ for the different traffic databases. The Swedish traffic generated the highest λ_{HFMI} for all Φ with a maximum difference of 1.9 % compared with the Dutch traffic from 2008, see Figure 5.1.

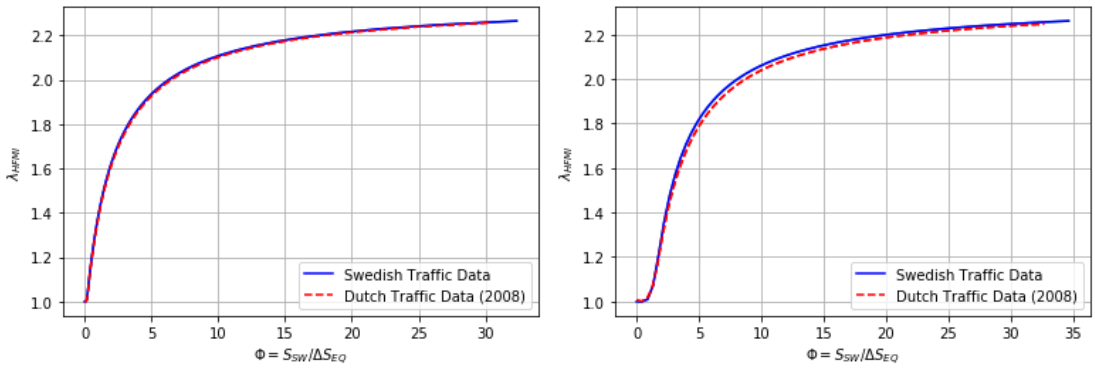

Figure 5.1 *Comparison of Φ-λ_{HFMI} curves calculated for real Swedish and Dutch traffic (2008). To the left: Mid-span section. To the right: Support sections.*

It can also be noted that the abnormal overload, in the database from 2018, does not affect the result in the same manner as before, see Figure 5.2. The Swedish traffic produced the highest λ_{HFMI} with the largest difference of 2.4 % which was found in the support section.

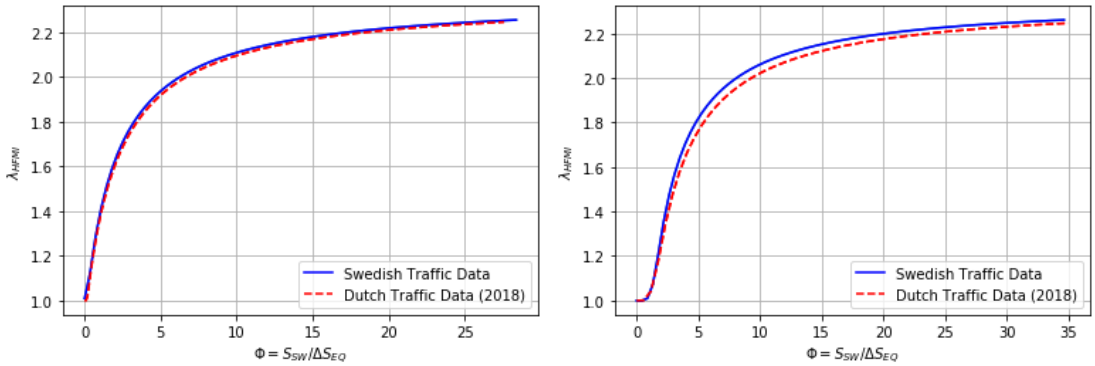

Figure 5.2 *Comparison of Φ-λ_{HFMI} curves calculated for real Swedish and Dutch traffic (2018). To the left: Mid-span section. To the right: Support sections.*

5.1.1 Design framework

The Swedish traffic generated the highest λ_{HFMI} in all cases. Therefore, it can be stated that the expressions for λ_{HFMI} in Equation (3.5) and (3.6) would also be valid for Dutch traffic. However, in this section, new expressions are derived for λ_{HFMI} for compatibility with the new definition of Φ. The expressions should be based on the results from the Swedish traffic data since it produced the highest λ_{HFMI}. A curve fit of the Φ-λ_{HFMI} curves, see Figure 5.3, resulted in one equation for mid-span sections, see Equation (5.2), and one equation for mid-support sections, see Equation (5.3).

$$\lambda_{HFMI} = \frac{2.36\phi + 2.00}{\phi + 2.15} \tag{5.2}$$

$$\lambda_{HFMI} = \frac{2.36\phi - 0.42}{\phi + 1.26} \tag{5.3}$$

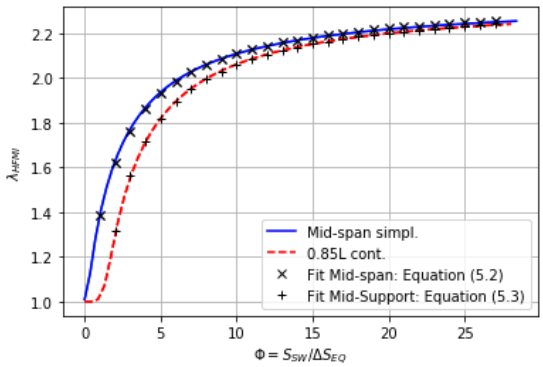

Figure 5.3 *Φ-λ_{HFMI} curves proposed for use in the design of mid-span and mid-support section.*

In order to calculate ϕ, Palmgren-Miner's equivalent stress range, ΔS_{eq}, needs to be known. Like the methodology in Chapter 4, the relationship to the stress range from FLM3, ΔS_p, is used which is a parameter known to the designer. There is no single constant that represents the ratio for all span lengths in a satisfactory manner, see Figure 5.4. Instead, a factor ξ is introduced, one for mid-span sections, Equation (5.4), and one for mid-support sections, Equation (5.5). This results in expressions where all parameters are known to the designer, see Equation (5.6).

$$\xi = 0.0045L + 0.55 \quad for \quad 10m \leq L < 55m \tag{5.4}$$
$$\xi = 0.80 \quad for \quad L \geq 55m$$

$$\xi = 0.0057L + 0.33 \quad for \quad 10m \leq L < 55m \tag{5.4}$$
$$\xi = 0.64 \quad for \quad L \geq 55m$$

$$\Phi = \frac{S_{sw}}{\xi \cdot \Delta S_p} \tag{5.6}$$

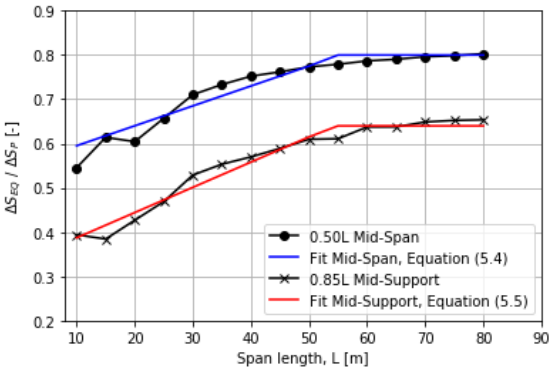

Figure 5.4 *The ratio of Palmgren-Miner's equivalent stress range, ΔS_{eq}, to the stress range from FLM3, ΔS_p.*

6 Prediction of λ_{HFMI} using fatigue load models

The results obtained in Chapter 4 and Chapter 5 have confirmed that the mean stress effect of HFMI-treated welds subjected to variable amplitude loading with varying mean stress can be predicted using the method proposed by Shams-Hakimi and Al-Emrani even for traffic from the Netherlands.

In this chapter, the Eurocode's [17] fatigue load model 3 and 4 were studied in terms of the mean stress effect. The aim was to investigate whether a fatigue load model can be used to obtain the factor λ_{HFMI} directly, without using Equation (3.5) and Equation (3.6).

For each load model, stress ranges were generated in the same manner as in Chapter 4 and 5 for span and support sections, however, in addition, a range of span lengths between 10 and 80 meters were investigated instead of only 10 meters. In order to obtain λ_{HFMI}, different approaches were needed for the two different load models.

For FLM4, Palmgren-Miner's equivalent stress range was calculated, according to Equation (3.2). Thereafter, each stress range was modified by the correction factor *f*, see Equation (3.1), in order to obtain the modified stress range, see Equation (3.3). Lastly, λ_{HFMI} was calculated as the ratio of Palmgren-Miner's equivalent stress range and the modified equivalent stress range, see Equation (3.4).

For FLM3, the stress ratio of the largest generated stress range ($\Delta S_{FLM3} = \Delta S_p$) was calculated and the correction factor, *f*, was obtained according to Equation (3.1). This correction factor was used as a representation of λ_{HFMI}, see Figure 6.1.

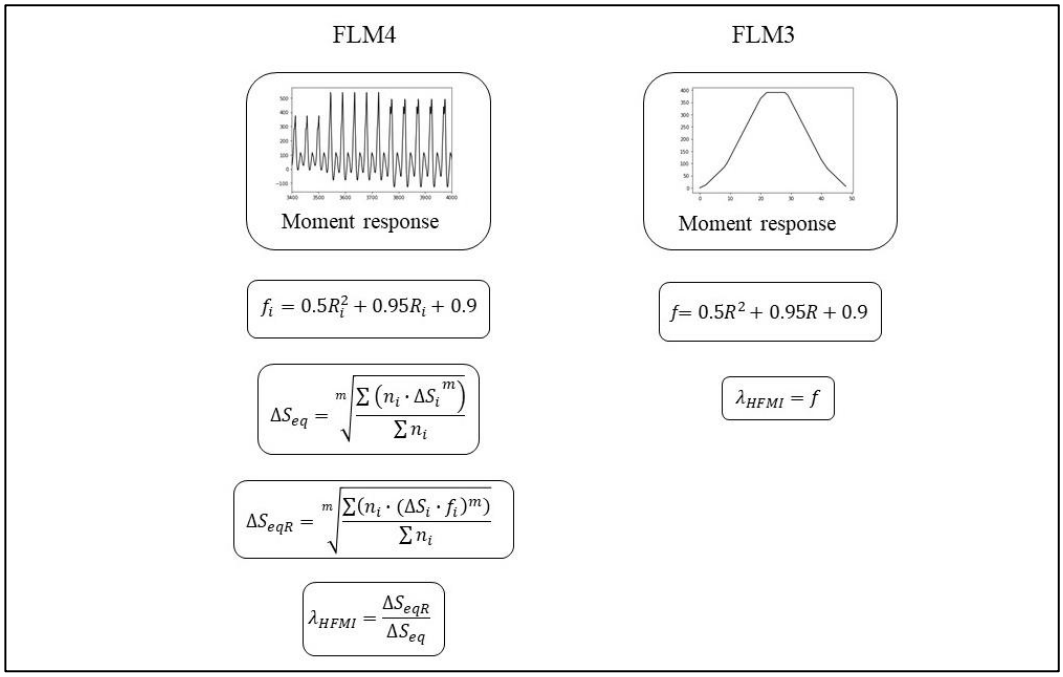

Figure 6.1 Illustration of the calculation procedure of λ_{HFMI} for FLM3 and FLM4.

6.1 Results

The calculated λ_{HFMI} for the different load models were compared with λ_{HFMI} for the real Swedish traffic data consisting of 872,091 vehicles, as the ratio $\lambda_{HFMI,real}/\lambda_{HFMI,loadmodel}$. The comparison was made for 0.50L and 0.85L, for different span lengths and self-weights. The self-weights were chosen to obtain R-ratios between 0.1 and 0.9 (for mid-span sections of a simply supported bridge).

6.1.1 FLM3

As can be seen in Figure 6.2, FLM3 predicts an underestimation of λ_{HFMI}, for nearly all self-weights and span-lengths. The discrepancy are largest for a span length of 10 meters and they increase with an increasing self-weight when $S_{SW} < \Delta S_p$ (R < 0.5). When S_{SW} becomes greater than ΔS_p (R > 0.5), the differences start decreasing with increasing self-weight. The mid-span and the support section have a maximum disparity of 6 % and 23 % respectively.

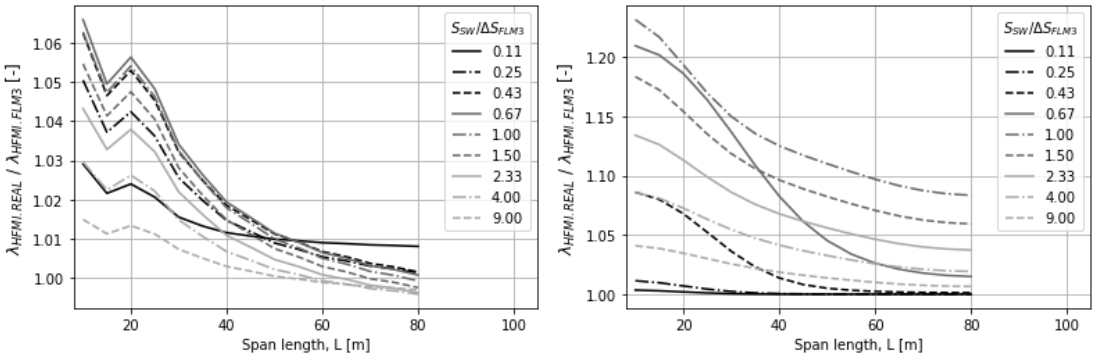

Figure 6.2 The ratio of λ_{HFMI} for real traffic and λ_{HFMI} for FLM3 calculated for mid-span section (to the left) and mid-support section (to the right).

6.1.2 FLM4

Figure 6.3 shows that the results obtained for FLM4, local traffic, follows a similar trend as for FLM3, were the discrepancy increases with increasing self-weight and starts decreasing for R > 0.5. It was also be revealed that FLM4, local traffic, made the best prediction, of λ_{HFMI}, of all the investigated fatigue load models. All results are conservative, for L < 25 m, in the mid-span section and, for L < 40 m, in the support-section. The largest underestimation of λ_{HFMI} was found, in the mid-support section, at a span length of 10 m.

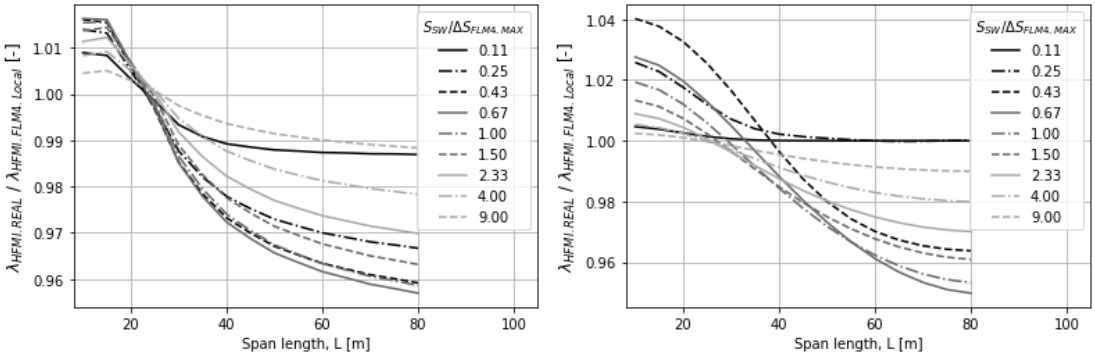

Figure 6.3 The ratio of λ_{HFMI} for real traffic and λ_{HFMI} for FLM4 (local traffic) calculated for mid-span section (to the left) and mid-support section (to the right).

As can be seen in Figure 6.4 and Figure 6.5, FLM4 medium distance and long distance obtained liberal results, for almost all cross-sections and span lengths. The largest discrepancy was found to be 10 %, in the mid-support section, for short span bridges.

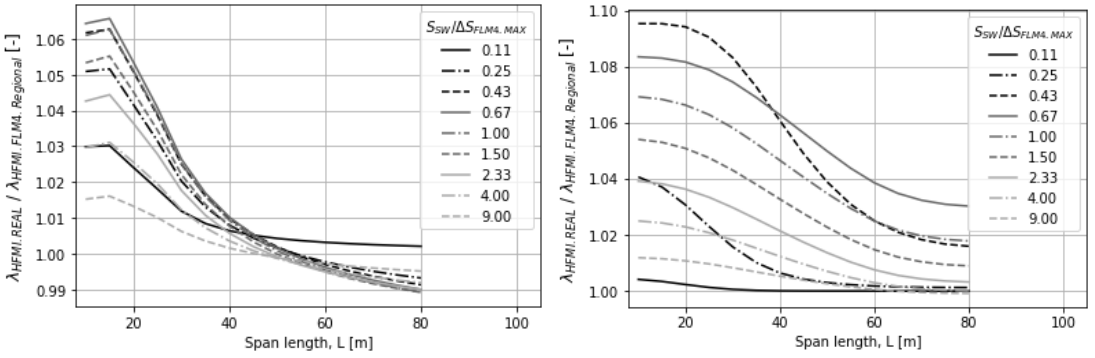

Figure 6.4 The ratio of λ_{HFMI} for real traffic and λ_{HFMI} for FLM4 (medium distance) calculated for mid-span section (to the left) and mid-support section (to the right).

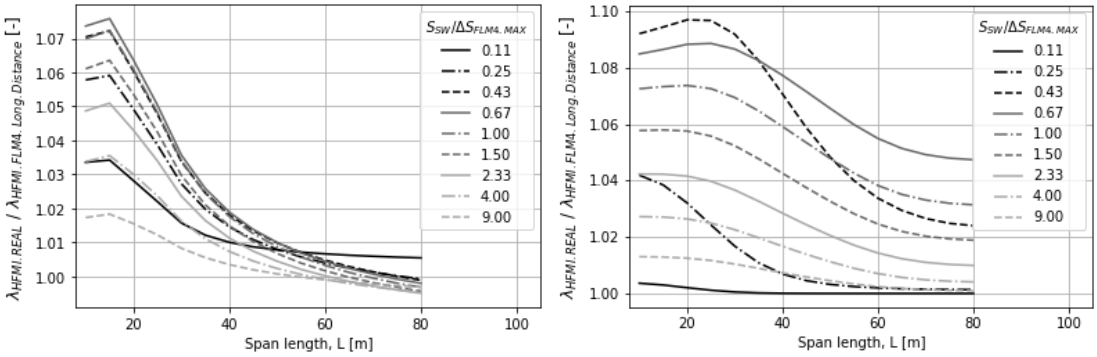

Figure 6.5 The ratio of λ_{HFMI} for real traffic and λ_{HFMI} for FLM4 (long distance) calculated for mid-span section (to the left) and mid-support section (to the right).

Figure 6.3 showed that FLM4, local traffic, obtained the best prediction of λ_{HFMI}. Therefore, further studies were performed for this fatigue load model. The ratios of λ_{HFMI} for real traffic and λ_{HFMI} for FLM4 (local traffic) were calculated for two types of continuous bridges with unequal span lengths to investigate a wider variety of bridge geometries. The first type was a three-span bridge with a middle span of $L_2 = 0.7L_1$, see Figure 6.6, whereas the second type was a three-span bridge with a middle span of $L_2 = 1.3L_1$, as can be seen in Figure 6.9.

Figure 6.7 and Figure 6.8 shows the prediction of λ_{HFMI} was more liberal compared with the results in Figure 6.3. The largest underestimation of λ_{HFMI} was found to be 10 % and was obtained for short span bridges, in the mid-span section of the middle span.

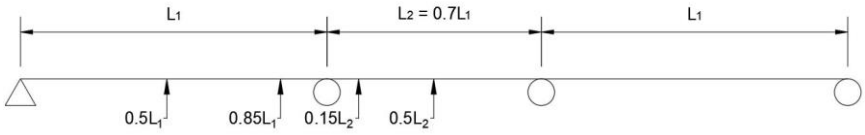

Figure 6.6 Geometry and investigated locations of the asymmetric bridge, with a shorter mid-span.

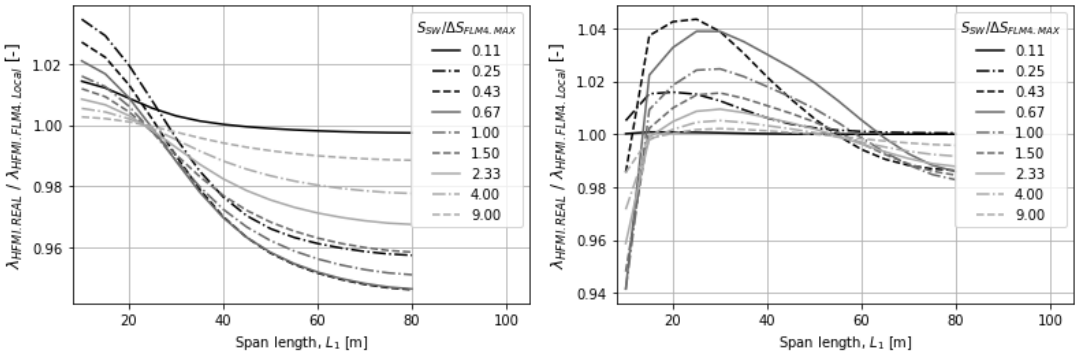

Figure 6.7 The ratio of λ_{HFMI} for real traffic and λ_{HFMI} for FLM4 (local traffic) calculated for $0.50L_1$ (to the left) and $0.85L_1$ (to the right).

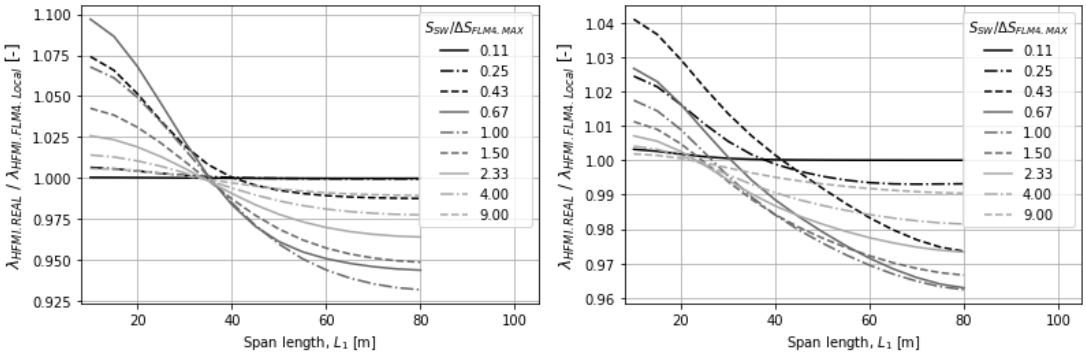

Figure 6.8 The ratio of λ_{HFMI} for real traffic and λ_{HFMI} for FLM4 (local traffic) calculated for $0.50L_2$ (to the left) and $0.15L_2$ (to the right).

Figure 6.10 and Figure 6.11 shows that the bridge with a longer mid-span obtained similar results as the symmetric two-span bridge, see Figure 6.3. The largest underestimation was 6 % and was found at $0.15L_2$.

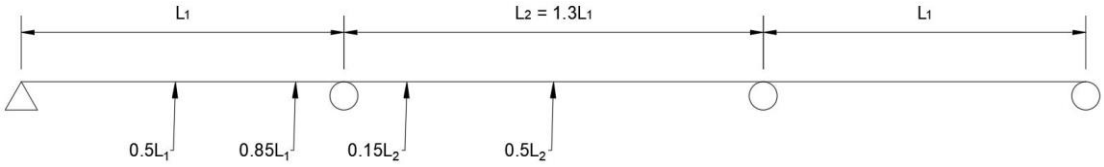

Figure 6.9 Geometry and investigated locations of the asymmetric bridge, with a longer mid-span.

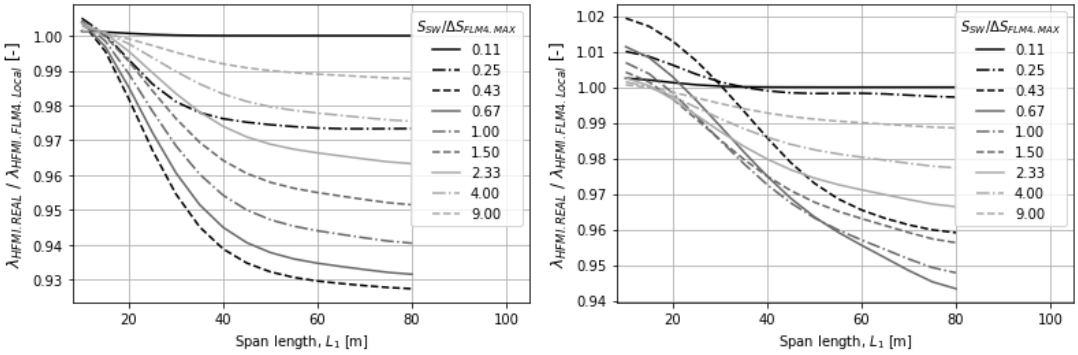

Figure 6.10 The ratio of λ_{HFMI} for real traffic and λ_{HFMI} for FLM4 (local traffic) calculated for $0.50L_1$ (to the left) and $0.85L_1$ (to the right).

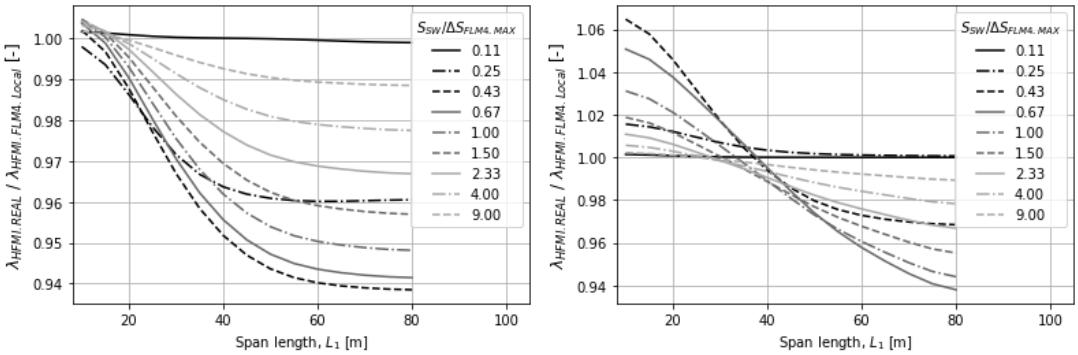

Figure 6.11 The ratio of λ_{HFMI} for real traffic and λ_{HFMI} for FLM4 (local traffic) calculated for $0.50L_2$ (to the left) and $0.15L_2$ (to the right).

7 λ_{HFMI} in case-study bridges

Previous chapters have studied the variation of λ_{HFMI}, in mid-span and mid-support sections for fictitious bridges. In this chapter, all the earlier investigated methods will be performed, in all cross-sections, on three different girder bridges that have been built in Sweden.

All the bridges, see Figure 7.1, are composite steel and concrete bridges which gives unfavorable conditions for HFMI-treated welds due to the high mean stresses from the self-weight. The bridges are adopted from Dr. Shams-Hakimi's Phd. thesis where more detailed information on the bridges has been published [3].

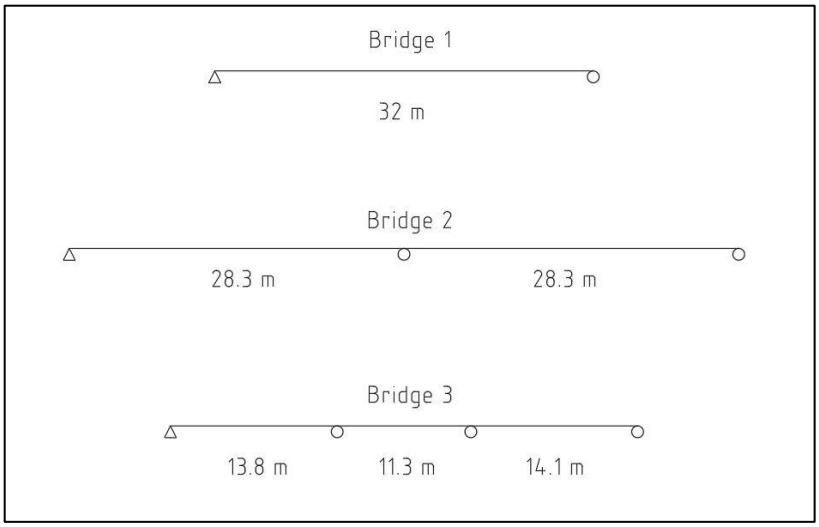

Figure 7.1 Span lengths for investigated bridges.

The calculations were carried out by only considering the moment variation along the bridges. The magnitude of λ_{HFMI} will, therefore, differ from the actual λ_{HFMI}-values, calculated with the real stress of the studied detail. However, the purpose of this study was to compare the relationship between all the earlier investigated methods and real traffic, which will remain the same. Bending moment influence lines were generated for all sections with a spacing of 1 meter. Variation in bending stiffness, due to cracking of the concrete deck and variations in the girder sections, were taken into account. The self-weight of the bridges was defined by the steel girders, concrete deck and paving to obtain realistic self-weights. The parameters used for the calculations is provided in Appendix A.

Bridge 1 is a 32 meter simply supported bridge. FLM4 and the design framework proposed by Shams-Hakimi and Al-Emrani [3][6] predict conservative λ_{HFMI} values for all cross-sections along the bottom flange of the bridge, see Figure 7.2. The modified design framework, presented in Section 5.1.1, generates a λ_{HFMI} that is equal or conservative to the real traffic. FLM3 predicts liberal λ_{HFMI} values along the whole beam. The top flange of the girder is in compression and all methods results in λ_{HFMI} = 1.0, see Figure 7.3.

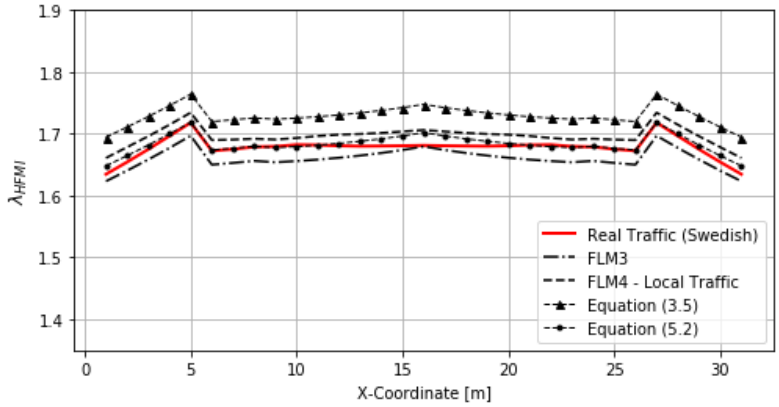

Figure 7.2 λ_{HFMI} calculated in the bottom flange of Bridge 1.

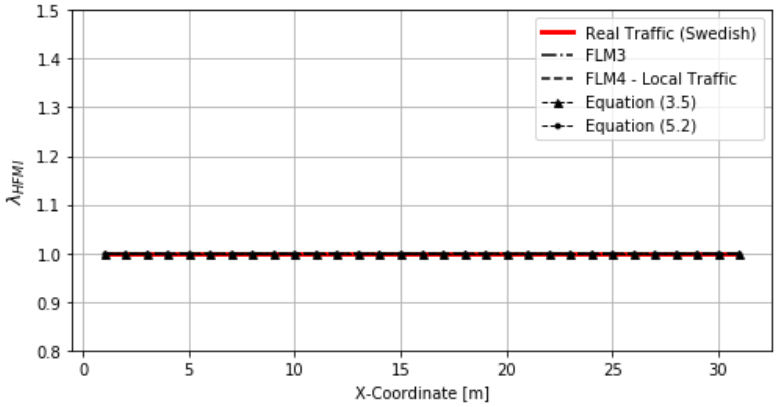

Figure 7.3 λ_{HFMI} calculated in the top flange of Bridge 1.

Bridge 2 is a symmetric two-span bridge with span lengths of 28.3 meters. All methods predict conservative λ_{HFMI} values, for the bottom flange, except from fatigue load model 3, see Figure 7.4. The same results are obtained for the top flange, see Figure 7.5.

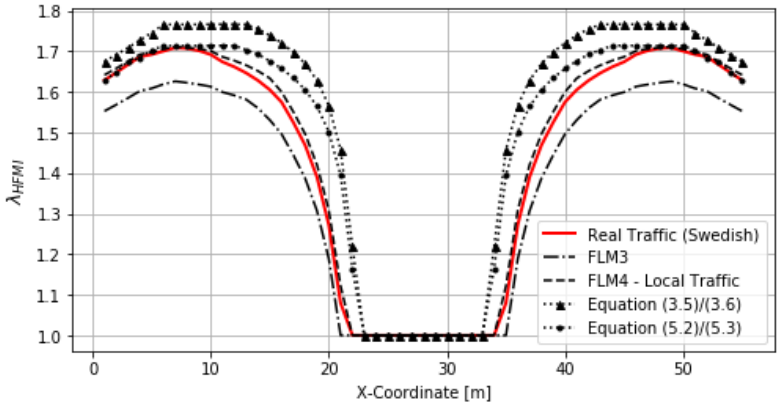

Figure 7.4 λ_{HFMI} calculated in the bottom flange of Bridge 2.

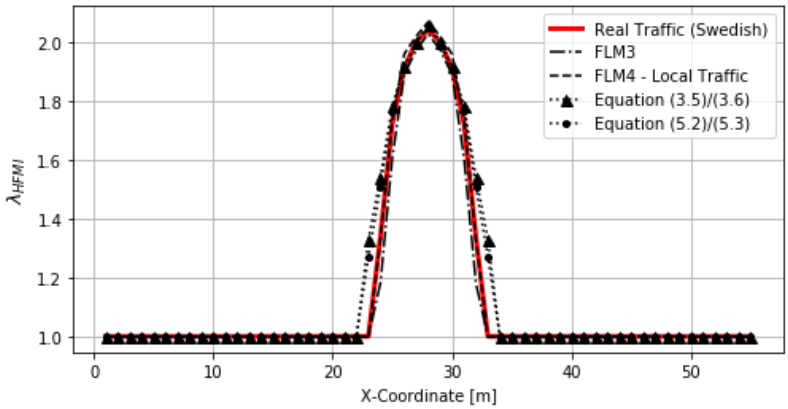

Figure 7.5 λ_{HFMI} calculated in the top flange of Bridge 2.

Bridge 3 consists of three continuous spans with a total length of 39.2 meters. The design framework proposed by Shams-Hakimi and Al-Emrani [3][6] and the modified method, presented in Section 5.1.1, give conservative results in both the bottom and top flanges, see Figure 7.6 and Figure 7.7. In contrast, FLM3 and FLM4 underestimate λ_{HFMI} in all cross-sections of the bottom flange. The largest difference is obtained in the middle-span where the fatigue load models obtain a constant value of λ_{HFMI} = 1.0.

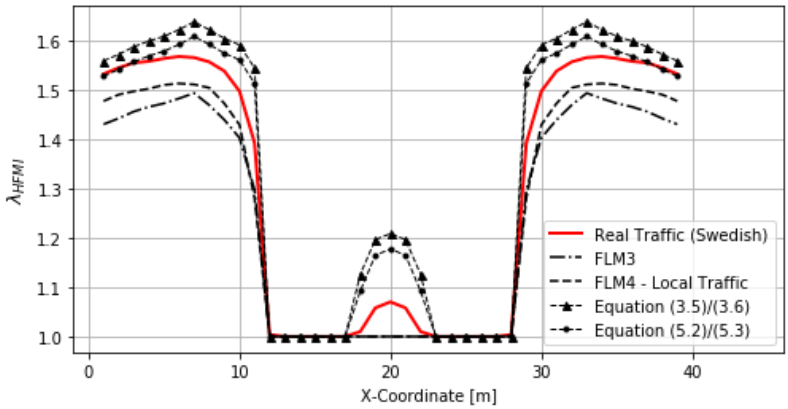

Figure 7.6 λ_{HFMI} calculated in the bottom flange of Bridge 3.

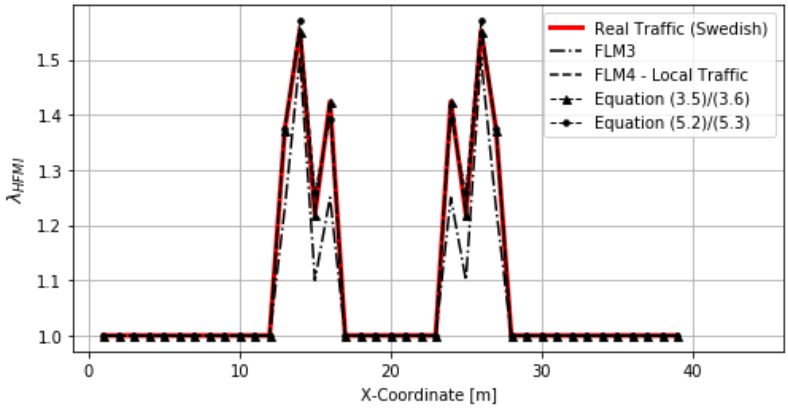

Figure 7.8 λ_{HFMI} calculated in the top flange of Bridge 3.

8 Discussion

The discussion is divided in to four parts, one for each Chapter 4, 5, 6 and 7.

8.1 Chapter 4 – Validity of the data

The traffic data base used by Shams-Hakimi and Al-Emrani [3][6], containing 55,000 Swedish trucks was shown to be enough to represent the traffic on Swedish roads in terms of the mean stress effect. The maximum discrepancy of 1.03 % compared with the larger data base of Swedish traffic is considered unimportant in this context.

Chapter 4 also showed that the method is applicable on Dutch road traffic. The Swedish traffic generated larger λ_{HFMI} for all Φ and is thereby conservative. This makes the Swedish traffic suitable as the basis for derivation of expressions for λ_{HFMI}. The similarities of the λ_{HFMI}-Φ curves for the two countries (Figure 4.3) can be explained by studying the stress range spectra, in Figure 4.2. The two spectra are relatively close to each other were the distribution of the stress ranges follow the same trends. However, it can be seen that the Swedish database contains a greater proportion of larger stress ranges compared with the Dutch traffic database. That could be explained by the fact that Sweden is one of the countries in Europe that allows the highest maximum weight of lorries [18] and this could be the reason why Swedish traffic produced a greater mean stress effect (2.6% higher lambda at most). The maximum permitted gross weight on Swedish and Dutch roads is 60 ton and 50 ton respectively.

Since the method is dependent on the maximum stress range, the comparison of different traffic pools will vary depending on the stress range produced by a single vehicle, which is not appropriate. The abnormal stress range in Figure 4.4 affected the λ_{HFMI}-Φ curves too much to give representative comparisons.

8.2 Chapter 5 – Improvements of the method

By redefining Φ as the ratio of the stress caused by the self-weight and Palmgren-Miner's equivalent stress range, the λ_{HFMI}-Φ curves are no longer dependent of only one vehicle and the problem of comparing different traffic pools can be overcome. The results in Figure 5.2 show that the maximum stress range does not affect λ_{HFMI} in the same manner. A comparison of Figure 5.1 and Figure 5.2 shows that the traffic data from 2018 generated lower λ_{HFMI} than the traffic data from 2008. This can be explained by the fact that the traffic data from 2018 had a lower equivalent stress range, even if it contained a larger maximum stress range.

The Swedish traffic data base generated larger λ_{HFMI} compared with the Dutch traffic data base, in both sections and for all Φ.

8.3 Chapter 6 – Prediction of λ_{HFMI} using fatigue load models

It was investigated whether Eurocode's fatigue load models 3 and 4 could be used as an alternative to the approaches in the previous chapters to account for the mean stress effect directly. An obvious benefit of this approach would be that no distinction

between span and support section would be required which could hopefully result in less conservative predictions of the mean stress effect.

FLM3 resulted in a maximum discrepancy of 6 % in mid-span sections compared with real traffic, which may considered to be acceptable. On the other hand, FLM3 gave a λ_{HFMI} that was up to 23 % smaller than λ_{HFMI} for real traffic. This gives a large underestimation of λ_{HFMI}. The greatest discrepancy was obtained, in support sections, for low self-weights. This is since a lower self-weight stress makes the R-ratio more sensitive to changes in the applied load. However, when the self-weight stress is low, the detailed geometry of the vehicles becomes more important, i.e. axle loads and axle distance. FLM3 is represented by only one vehicle which is not enough to represent real traffic in mid-support sections.

FLM4, which contains five different vehicles, represented the real traffic in a better manner than FLM3. FLM4, local traffic, was the fatigue load model that resulted in the best agreement with the real traffic. The maximum discrepancy was, for all three traffic types, found in the mid-support section. In Figure 6.3, it can be seen that the largest disparity was obtained for $S_{sw}/\Delta S_{FLM4} = 0.43$. Why the discrepancy was smaller for lower self-weight proportions can be explained by the R-ratio limit of 0.1. $S_{SW} < 0.43$ caused the majority of the stress cycles to have an R-ratio < 0.1, resulting in a correction factor $f = 1.0$ for these cycles for both the fatigue load model as well as the real traffic.

FLM3 and FLM4 medium- and long-distance traffic underestimated λ_{HFMI} in all sections and for almost every span length. That results in a prediction of the mean stress effect that is unsafe. In contrast, FLM4 local traffic resulted in conservative predictions of λ_{HFMI} for all span lengths of $L > 20$ m in mid-span sections and all $L > 40m$ in mid-support sections. Anyhow, there is a maximum underestimation of 4 %, found in the mid-support section with a span length of 10 meter. The discrepancy is small could be considered acceptable.

In order to cover a greater verity of bridge geometries, two different, asymmetric, three-span bridges were investigated. It could be seen, in Figure 6.8, that the largest underestimation of λ_{HFMI} increased to 10 %. The most considerable discrepancy was found in the mid-span section of the middle support. Again, the smaller middle support results in lower self-weight stress, compared with the earlier studied bridges, which makes the R-ratio more sensitive for changes in the applied load.

Figure 7.1 shows a comparison of the normalized stress range spectrum of the larger Swedish traffic pool, as a cumulative frequency distribution, compared with the different traffic types of FLM4. It can be seen that the local traffic generates the stress range spectrum with a distribution closest to the Swedish traffic. This is suspected to be the reason why the local traffic is the traffic type that predicts λ_{HFMI} best.

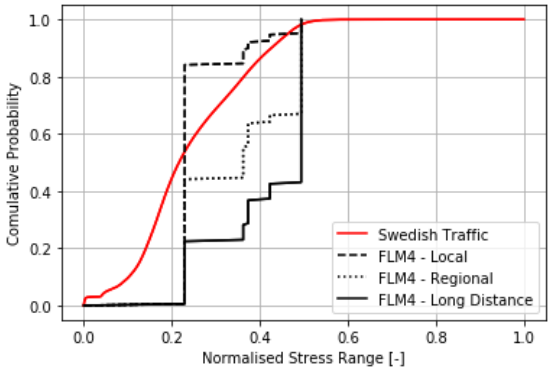

Figure 7.1 Normalised stress range spectrum as a cumulative frequency distribution.

8.4 Chapter 7 - λ_{HFMI} in case-study bridges

In Chapter 7, all methods presented in this thesis were used to predict λ_{HFMI} for three different case-study bridges. The results were compared with the real λ_{HFMI} values coming from the larger Swedish traffic pool/data base.

It could be seen that FLM3 obtained liberal λ_{HFMI} values, in all cross-sections, for all bridges. However, it should be noticed that the predicted values were still close to the real λ_{HFMI} values, in most of the cross-sections, for all bridges. FLM4, local traffic, obtained an even closer prediction. The results from bridge 1 and 2, see Figure 7.2-7.5, showed that FLM4 generates conservative or equal λ_{HFMI} values in all cross-sections. On the other hand, for Bridge 3, were liberal results obtained. The prediction gave an underestimation, in all cross-sections, along the bottom flange of the beam. The most inadequate estimation was found in the second span where the estimated values deviated from the trend of the real values. This corresponds well with the study of the three-span bridge, with a smaller middle span, presented in Chapter 6 (Figure 6.6), were the most considerable prediction was obtained in the mid-span section of the middle span, see Figure 6.8.

The method suggested by Shams-Hakimi and Al-Emrani [3][6], presented in Section 3.2.3.1, and the modified method, from Section 5.1.1, gave a good estimation of λ_{HFMI} for all the three case-study bridges. The results are conservative or equal to the real λ_{HFMI}, in all sections along the bridges. The modified equation obtains values that are closer to the real λ_{HFMI}. This is since the stress range from FLM3 is multiplied by the factor ξ, which varies with the span length, see Figure 5.4. In contrast, the method, from Section 3.2.3.1, is using a constant factor of 2.0, independently of the span-length, see Figure 3.5. This results in a more considerable discrepancy when the ratio between ΔS_{max} and ΔS_p increases.

9 Conclusions

This thesis aimed to study realistic load effects on HFMI-treated bridges and to investigate different methods to predict the impact of the mean stresses on the performance of HFMI-treated welds. 1) Studies were conducted on the validity of Shams-Hakimi and Al-Emrani's [6][3] method for prediction of the mean stress effect of HFMI-treated joints in bridges and 2) the applicability of the method on Dutch traffic data was investigated. Alternative design frameworks for HFMI-treated joints were investigated, 3), one method based on a modification of the proposal by Shams-Hakimi and Al-Emrani [6][3] and, 4), one method based on the direct use of Eurocode's fatigue load models. Based on these outcomes, 5), the validity of all the methods was studied on case-study bridges. Based on work in this thesis, the following conclusions can be drawn.

- It was shown that the traffic data pool, used by Shams-Hakimi and Al-Emrani in order to predict the mean stress effect for HFMI-treated joints in bridges, is representative for Swedish road traffic. An increase of the traffic data pool by 1500% did not affect the results.

- The method suggested by Shams-Hakimi and Al-Emrani is also applicable for Dutch traffic. The results obtained from the Swedish traffic showed a small conservativity to the Dutch results, which together with the fact that Sweden is one of the countries that allows the highest maximum gross-weight, strengthen the procedure of basing the method on Swedish traffic data.

- In this thesis, a modified version of the original design framework is proposed. The modification resulted in less conservative and more accurate predictions of the mean stress effect.

- An investigation of the Eurocode's fatigue load model 3 and 4 showed that FLM4 local traffic is the fatigue load model that gives the best prediction of the mean stress effect of HFMI-treated joints in bridges.

- A verification of all the methods was performed on three case-study bridges. Both the method proposed by Shams-Hakimi and Al-Emrani and the modified version obtained conservative and reasonable results for all three bridges. It was shown that the modified method predicts values closer to real traffic.

9.1 Suggestions for further research

For future work, the following subjects are suggested.

- Using the modified design framework on real in-service measurements from bridges to investigate the validity of the method.

- Using the proposed design framework to develop expressions to consider the mean stress effect in railway bridges.

10 References

[1] Al-Emrani, M., Åkeström, B. (2013): *Steel Structures.* Report 2013:10, Department of Civil and Environmental Engineering, Chalmers University of Technology, Gothenburg, Sweden, 2013.

[2] Dahlvik, M., Eriksson, J. (2014): *Load Effect Modelling in Fatigue Design of Composite Bridges.* Master's Thesis, Royal Institute of Technology (KTH), Stockholm, Sweden, 2014.

[3] Shams-Hakimi, P. (2020): *Fatigue improvement of steel bridges with high-frequency mechanical impact treatment.* Ph.D. Thesis, Chalmers University of Technology, Gothenburg, Sweden, 2020.

[4] Mosiello, A., Kostakakis, K. (2013): *The benefits of Post Weld Treatment for cost efficient and sustainable bridge design.* Master's Thesis, Chalmers University of Technology, Gothenburg, Sweden, 2013.

[5] Marquis, G. B., Barsoum, Z. (2016): *IIW Recommendations for HFMI Treatment - For Improving the Fatigue Strength of Welded Joints.* Singapore: Springer Singapore, 2016.

[6] Shams-Hakimi, P., Al-Emrani, M. (2020): *High-cycle variable amplitude experiments and a design framework for bridge welds treated by high-frequency mechanical impact.* Submitted to Engineering Structures, 2020.

[7] Eurocode 1, *Actions on structures – Part 2: Traffic loads on bridges.* European Committee for Standardization, 2003.

[8] Al-Emrani, M., Aygül, M. (2014): *Fatigue design of steel and composite bridges.* Report 2014:10, Chalmers University of Technology, Gothenburg, Sweden, 2014.

[9] Kirkhope, K. J., Bell, R., Caron, L. and Basu, R. I. (1996): *Weld Detail Fatigue Life Improvement Techniques (No. SR-1379).* MIL Systems Engineering, Ottawa, Canada, SR-1379, 1996.

[10] Hobbacher, A. (2008): *Recommendations for Fatigue Design of Welded joints and Components.* International Institute of Welding, doc. XIII-2151r4-07/XV-1254r4-07, Paris, France, 2008.

[11] Lindqvist, S., Holmgren, J. (2007): *Alternative Methods for Heat Stress Relief.* Master's Thesis, Luleå University of Technology, Luleå, 2007.

[12] Marquis, G. B., Mikkola, E., Yildirim, H. C., Barsoum, Z. (2013): *Fatigue strength improvement of steel structures by high-frequency mechanical impact: proposed fatigue assessment guidelines,* Weld World, vol. 57, no. 6, pp. 803-822, Nov. 2013.

[13] Mikkola, E., Dore, M., Khurshiad, M. (2013): *Fatigue strength of HFMI treated structures under high R-ratio and variable amplitude loading.* Procedia Engineering, vol. 66, pp. 161-170, 2013, doi: 10.1016/j.proeng.2013.12.071.

[14] Eurocode 3, *Design of steel structures – Part 2: Steel bridges.* European Committee for Standardization, 2006.

[15] Leander, J. (2017): *Kalibrering av lambda-metoden för dimensionering av stål- och samverkansbroar I Sverige – en förstudie.* KTH Royal Institute of Technology, Stockholm, 2017.

[16] Maljaars, J. (2019): *Evaluation of traffic load models for fatigue verification of European road bridges.* Submitted for publication in ENG Struct, 2019.

[17] Eurocode 1, *Actions on structures – Part 2: Traffic loads on bridges.* European Committee for Standardization, 2003.

[18] Sundquist, H. *Laster och lasteffekter av trafik på broar – Litteraturstudie.* Technichal Report nr. 98:66, KTH Royal Institute of Technology, Stockholm.

Appendix A

Properties of the case-study bridges

All values are adopted from Dr. Shams-Hakimi's Phd. thesis [3].

Loads

Self-weight loads per I-beam.

Bridge	Steel [kN/m]	Concrete [kN/m]	Pavement [kN/m]
1	3.7	22	6.15
2	4.4	43	10.1
3	2.8	26	8.9

Proportion of traffic load in the investigated beam.

Bridge	LDF
1	0.833
2	1.140
3	1.106

Cross section constants

Bridge 1:

Moment of inertia (short-term)

Coordinate [m]	0-9	9-23	23-32
I [m^4]	0.0427	0.0495	0.0427

Bridge 2:

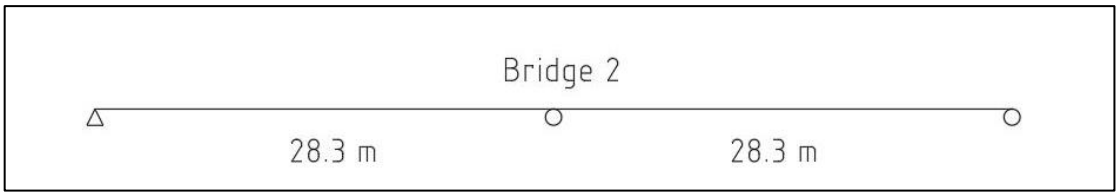

Moment of inertia (short-term)

Coordinate [m]	0-7	7-24	24-36.6	32.6-49.6	49.6-56.6
I [m^4]	0.049	0.055	0.026	0.055	0.049

Bridge 3:

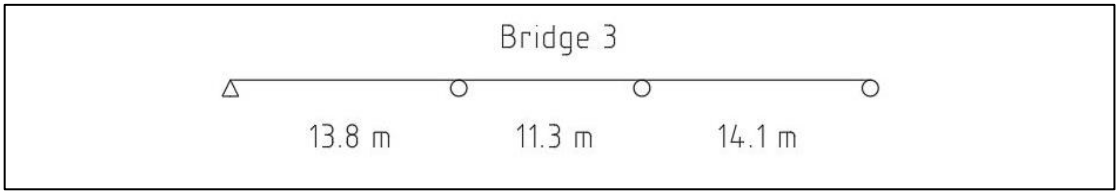

Moment of inertia (short-term)

Coordinate [m]	0-10.365	10.365-11.745	11.745-15.51	15.51-16.64	16.64-22.29	22.29-23.42	23.42-27.11	27.11-28.435	28.435-39.2
I [m^4]	0.010	0.008	0.003	0.008	0.009	0.008	0.003	0.008	0.009

DEPARTMENT OF ARCHITECHTURE AND CIVIL ENGINEERING
DIVISION OF STRUCTURAL ENGINEERING
CHALMERS UNIVERSITY OF TECHNOLOGY
Gothenburg, Sweden
www.chalmers.se

CHALMERS
UNIVERSITY OF TECHNOLOGY